RESEARCH MEMORANDUM

A FLIGHT COMPARISON OF A SUBMERGED INLET AND A SCOOP INLET AT TRANSONIC SPEEDS

By L. Stewart Rolls

Ames Aeronautical Laboratory
Moffett Field, Calif.

CLASSIFIED DOCUMENT

This material contains information affecting the National Defense of the United States within the meaning of the espionage laws, Title 18, U.S.C., Secs. 793 and 794, the transmission or revelation of which in any manner to an unauthorized person is prohibited by law.

NATIONAL ADVISORY COMMITTEE
FOR AERONAUTICS

WASHINGTON

March 19, 1953

NACA RM A53A06

NATIONAL ADVISORY COMMITTEE FOR AERONAUTICS

RESEARCH MEMORANDUM

A FLIGHT COMPARISON OF A SUBMERGED INLET AND A SCOOP INLET AT TRANSONIC SPEEDS

By L. Stewart Rolls

SUMMARY

Flight tests were conducted on two different inlet configurations, a submerged divergent-wall inlet, and a scoop inlet to determine their characteristics when installed on a YF-93 airplane. Measurements were made of the pressure-recovery characteristics of the inlets and the over-all airplane drag for each configuration. The submerged inlet had higher pressure recoveries throughout most of the Mach number range, but also had higher drag than the scoop inlet below 0.89 Mach number. Compared on the basis of a factor of relative effectiveness, the two inlet installations were found to be of about equal merit and the maximum level flight Mach number at 25,000 feet altitude of the airplane was about the same for each inlet.

The boundary-layer bleeds used with these inlets were found to have considerable effect on the inlet operation. For Mach numbers below about 0.85, sealing the boundary-layer bleeds on the scoop inlet improved the low recoveries; whereas sealing the bleeds on the submerged inlets decreased the airplane drag coefficient.

INTRODUCTION

Preliminary flight tests on the YF-93 airplane equipped with a submerged inlet indicated its performance was considerably below the design estimates. During subsequent investigations, performed by the manufacturer, flight tests were made on a similar airplane which contained a different inlet configuration of the scoop type and a fuselage with a smaller aft end. The performance of the airplane was improved by these modifications. Since the results of this investigation were not sufficient to determine to what extent the inlet change contributed to the performance increase, the subject tests were initiated.

The purpose of the investigation presented in this report was confined to a determination of the pressure recovery and drag characteristics for each of the two inlet configurations. The two types of inlets tested were an NACA submerged divergent-wall (flush) inlet (fig. 1) and a scoop inlet (fig. 2). The scope of the investigation covered tests of the inlets in the Mach number range of about 0.50 to 0.98 and over the mass-flow-ratio range available by varying engine speeds from idle to full power. The results have been used to compare the inlet installations on three bases: (1) the induction-system efficiency (ram-recovery ratio at the inlet and at the compressor, and engine power output), (2) the over-all airplane drag coefficient, and (3) a computed factor of relative effectiveness.

NOTATION

A	inlet area, sq ft
A_L	acceleration factor along airplane body axis, positive for increasing forward velocity, $\frac{\text{longitudinal force}}{\text{airplane weight}}$
A_N	acceleration factor normal to airplane body axis, $\frac{\text{normal force}}{\text{airplane weight}}$ (An acceleration factor of 1 corresponds to 1 g.)
C_D	airplane drag coefficient, $C_c \cos \alpha + C_N \sin \alpha$
C_N	airplane normal-force coefficient, $\frac{WA_N}{q_o S}$
C_c	airplane longitudinal-force coefficient, $\frac{F_n - WA_L}{q_o S}$
D	total airplane drag, lb
F_g	gross engine thrust, lb
F_n	net engine thrust, lb
H	total pressure, lb/sq ft
M	Mach number
S	wing area, sq ft
V	airplane velocity, ft/sec
W	airplane weight, lb

[redacted]

g	acceleration due to gravity, 32.2 ft/sec^2
p	static pressure, lb/sq ft
q	dynamic pressure, lb/sq ft
w_a	rate of air flow into compressor, lb/sec
α	airplane angle of attack, deg
δ	$\frac{\text{average total pressure at face of compressor}}{\text{absolute static pressure of NACA standard atmosphere at sea level}}$
ρ	density, lb/cu ft

Parameters

$H-p_o/H_o-p_o$	ram-recovery ratio
m_1/m_o	mass-flow ratio, $w_a/\rho_o A_1 V_o$

Subscripts

o	free stream
1	inlet entrance station
2	compressor face

DESCRIPTION OF AIRPLANES

The pertinent dimensions of the YF-93 airplanes are listed in table I. Photographs of the test airplanes are shown in figures 1 and 2, and a two-view drawing of the airplane with submerged inlets is shown in figure 3.

Close-up views of the submerged and the scoop inlets are presented in figure 4. The inlet shapes and profiles are shown in figures 5(a) and 5(b), respectively, and the variations of cross-sectional-area distribution within the diffuser are shown in figure 5(c). The

different entrance areas, based on one inlet and exclusive of the boundary-layer bleeds, are 240 square inches for the submerged inlet and 215 square inches for the scoop inlet.

Location of the inlets and the boundary-layer bleed exits is shown in figure 6. Both inlets were equipped with boundary-layer bleed ducts which removed the boundary-layer air at the inlets and discharged it at exits on the fuselage aft of the inlets. In the case of the submerged inlet the exit spilled the boundary-layer air at right angles to the air flow over the fuselage, as shown by the arrow, while the exit on the scoop inlet spilled the air parallel to the external air flow.

Figure 6 also shows that the entrance of the scoop inlet was farther forward on the fuselage than that of the submerged inlet, resulting in a diffuser length of 14.6 feet compared to 10.0 feet for the submerged-inlet diffuser. Both diffusers dumped into the identical plenum chamber. The identical centrifugal-compressor engine (Model J-48-1) was used interchangeably in both airframes.

INSTRUMENTATION AND TESTS

Standard NACA recording instruments and a recording oscillograph synchronized at 1/10-second intervals by a single timing circuit were used to record the test data. True Mach numbers were calculated from measurements of total and static pressures obtained with a 12.5-foot nose boom. A calibration of this airspeed installation was obtained by the "fly by" method up to 0.88 Mach number. This calibration was extrapolated to higher Mach numbers by using the results of reference 1 and data obtained during the passage of the fuselage bow wave over the static orifices on the airspeed head at high Mach numbers.

During each test the left inlet was instrumented with a rake of total- and static-pressure tubes at a station 10 inches down the duct from the minimum area station shown in figure 5(b). The rake in the submerged inlet, visible in figure 4(a), had 45 total and 4 static tubes, while the rake in the scoop inlet had 32 total and 4 static tubes. The instrumentation in the plenum chamber used to measure the pressure recoveries at the compressor face consisted of five shielded total-pressure tubes.

The technique used to obtain total airplane drag by measurement of the engine thrust and airplane normal and longitudinal accelerations is discussed in the appendix.

The data presented in this report were obtained during runs at various power settings at constant Mach number in order to obtain varying mass-flow ratios. The range of test altitudes during the tests was 22,000 to 27,000 feet.

The precision of the measurements estimated from the least count of the instruments and the scatter and repeatability of the data are:

Mach number	±0.01
Ram-recovery ratio	±0.01
Pressure altitude	±150 ft
Drag coefficient	±0.0005
Thrust coefficient	±0.0003
Mass-flow ratio	±0.02

RESULTS AND DISCUSSION

Induction-System Efficiency

Ram-recovery-ratio characteristics.- The ram-recovery-ratio characteristics (the ratio of the impact pressure recovered to the impact pressure available ($H-p_o/H_o-p_o$)) were obtained from the survey-rake total-head tube pressures. The individual pressure readings were integrated over the area of the duct to determine the ram-recovery ratio, which was then plotted as a function of mass-flow ratio[1] at constant Mach number. Typical curves of the variation of ram-recovery ratio at the inlet and the compressor face with mass-flow ratio are presented in figures 7 and 8 for Mach numbers of 0.6, 0.7, 0.8, and 0.9. Curves of this type were then used to establish the variation of ram-recovery ratio with Mach number at constant values of mass-flow ratio.

Figure 9 is a comparison of the ram-recovery ratios at the inlet entrance for the submerged and the scoop inlet for mass-flow ratios of 0.6 and 0.8. The submerged inlet had higher recovery characteristics at the lower Mach numbers; however, the scoop-inlet recoveries were equal or superior above a Mach number of approximately 0.8. The pressure

[1]The mass-flow ratio as used in this report is the ratio of the weight of air entering the compressor to the weight of air at free-stream condition flowing through an area equal to the inlet area. The weight of air entering the compressor was determined from available curves of air flow versus engine speed and was checked by measurements of the exit gas flow.

recovery at lower Mach numbers for the scoop inlet is lower than would be predicted from wind-tunnel tests of a somewhat comparable installation (ref. 2). The measurements of the individual rake tubes in the scoop inlet indicated a uniformly low pressure recovery over the entire inlet. The total-pressure ratios H/H_o obtained at a station 3 inches ahead of the scoop lip (fig. 10) indicate no large separation losses forward of this point; the low inlet recovery of the scoop inlet thus is attributable to losses occurring at the inlet entrance. It appeared probable that the cause of these losses was the boundary-layer bleed.

A brief series of additional tests were conducted to determine if sealing the boundary-layer bleed (as shown in fig. 11) would reduce the entrance losses. These additional tests were made with a single rake of total-head tubes mounted at the center of the duct at the same duct station as the original 32-tube rake. The results with boundary-layer bleed sealed and unsealed are compared in figure 12; these results confirm the assumption that the boundary-layer bleed was the cause of the excessive losses at the lower Mach numbers.[2] With the boundary-layer bleeds sealed the expected duct instability (rumble) was obtained at low mass-flow ratios.

Recovery at the face of the compressor.- The pressure-recovery characteristics at the face of the engine compressor based on the average of the five total-head tubes are shown in figure 13. As a result of aforementioned high entrance losses, the scoop inlet gives considerably lower ram recovery at the compressor face at the lower Mach numbers than the submerged inlet installation. The data for the recoveries at the compressor face with the scoop-inlet boundary-layer bleeds sealed and unsealed are presented in figure 14. Comparison of the improvement in recovery at the compressor face with that measured at the inlet (fig. 12) indicates that there was less improvement at the compressor than at the inlet. This could possibly be due to allowing the boundary layer from the forward portion of the fuselage to flow into the inlets.

A comparison has been made with other available flight data on scoop inlets[3] to determine how the characteristics of the inlets on the

[2]All the data discussed in this section were obtained for the left inlet. A small amount of data obtained with a center-line rake for the scoop inlet on the right side indicates some difference between the left and right inlets. However, the over-all effects, that is, the large losses for the inlet and the beneficial effects of sealing the boundary-layer bleed, were also noticed on the right inlet.

[3]The data used were supplied through the courtesy of the Lockheed Aircraft Company in cooperation with the NACA Subcommittee on Internal Flow.

YF-93 airplanes compare with other installations. The comparison shown in figure 15 indicates that the recoveries measured at the compressor face of the YF-93 are typical of those that exist in the lower Mach number range for other scoop-inlet installations. It is to be observed that all airplanes involved in this comparison have centrifugal compressor engines and thus are confronted with a somewhat similar diffusion problem.

Engine power output.- In order to indicate directly the effects of the differences in the inlet-diffuser recoveries for the two inlet installations, a comparison of the engine power output has been included. The engine output which is a direct function of the recoveries at the compressor face was determined by two methods: First, the output was computed using the pressure recoveries at the compressor face and the manufacturer's estimated performance curves; and second, the output was measured at the exit of the engine tailpipe by using a single pressure probe. The equation for the thrust based on conditions in the tailpipe is presented in the appendix. The difference between the thrust output for the two inlet systems as determined from inlet-recovery data and from measurements at the tailpipe exit is presented in figure 16. The variation shown by these curves indicates that the difference in the thrust for the two inlet installations is as would be expected from the difference in pressure recovery.

Airplane Drag

The variation of airplane drag coefficient with Mach number for both inlet configurations at a normal-force coefficient of 0.15 is presented in figure 17. The data in figure 17 were used for deriving drag increments and do not represent the drag of the clean production airplane because of the presence of external test equipment and of the assumption of a tailpipe nozzle discharge of unity instead of a calibrated value. Also, the values of gross thrust used in the drag equation (see appendix) are those based on conditions at the tailpipe exit, not those at the extreme aft end of the fuselage. Thus the thrust losses, if any, associated with the afterburner cooling-air ejector are attributed to and appear in figure 17 as airplane drag. It is emphasized, however, that the test equipment, jet engine, and the complete fuselage aft-end assembly were identical for each inlet configuration and comparisons of drag increments are therefore valid.

The incremental difference in airplane drag coefficient between the submerged- and the scoop-inlet installations is presented in figure 18. The drag coefficient with the scoop inlet was 0.0030 less than that with

the submerged inlet below 0.84 Mach number. Above 0.89 Mach number the submerged-inlet configuration had the lower drag.

Tuft studies as well as tests by the airplane manufacturer indicated that one possible explanation for the higher drag with the submerged-inlet installation at low speeds was the effect on the air flow over the fuselage of exhausting the boundary-layer air at right angles to the air stream (see fig. 6). To check this the airplane drag coefficient with the submerged inlet was also measured with the boundary-layer bleed entrances and exits sealed in the way shown in figure 19. The drag coefficients with and without the bleed sealed (fig. 20) show a difference in drag coefficient of 0.0015 at 0.78 Mach number. Thus about half the drag difference for the two airplanes was due to the method of discharging the boundary-layer bleed air on the airplane with the submerged inlet.

It is also of interest to note, as indicated in figure 21, that sealing the existing boundary-layer bleed had only a small effect on the submerged-inlet pressure-recovery characteristics.

Relative Comparison of the Inlet Installations

To obtain a comparison of the over-all effectiveness of the two inlet installations the thrust differences and the drag differences were combined on one curve. This was done for a standard altitude of 25,000 feet by using the following parameter (the thrust in this equation was the thrust at the tailpipe exit measured while the drag was being determined):

$$\frac{(\text{gross thrust} - \text{drag})_{\text{submerged}} - (\text{gross thrust} - \text{drag})_{\text{scoop}}}{\text{rated gross thrust at 25,000 feet altitude}}$$

which is shown as a function of Mach number in figure 22. The comparison of the two curves indicates that the two inlets were of approximately equal merit, the differences being of the order of the experimental scatter of the thrust and drag measurements.

As a further comparison of the thrust and drag characteristics, the performance of the airplane (without afterburning) with each inlet installation was computed at a fixed altitude of 25,000 feet. The variations of thrust and drag coefficient with Mach number are shown in figure 23. The noted intersections of the thrust- and drag-coefficient

curves indicate about the same maximum-level-flight Mach number with each inlet configuration.

SUMMARY OF RESULTS

Flight tests conducted on the YF-93 airplane equipped with two different inlets, submerged divergent-wall inlets in one case and scoop inlets in the other, indicated the following:

1. Low ram-recovery ratios were measured for the scoop installation at both the inlet and at the compressor face at the lower Mach numbers. Sealing of the boundary-layer bleed ducts on the scoop inlet improved these low recoveries at the lower Mach numbers. These recoveries were lower than those measured for the submerged-inlet installation at Mach numbers below about 0.85.

2. Below about 0.84 Mach number the airplane drag coefficient was lower with the scoop inlet than with the submerged inlet. Sealing the boundary-layer bleed air ducts on the submerged inlet decreased this drag difference.

3. Compared on the basis of a factor of relative effectiveness at an altitude of 25,000 feet, the two inlets were of approximately equal merit and the maximum-level-flight Mach number, without afterburner, was approximately the same; thus the difference in the inlet configurations in this case had little effect on the performance of this airplane.

Ames Aeronautical Laboratory,
National Advisory Committee for Aeronautics,
Moffett Field, Calif.

APPENDIX

THE DETERMINATION OF DRAG

The drag as presented in this report was determined from the following equation:

$$D = W (A_N \sin \alpha - A_L \cos \alpha) + F_n \cos \alpha$$

where

D drag of airplane, lb

W weight of airplane, lb

A_N normal acceleration factor

A_L longitudinal acceleration factor

α angle of attack, deg

F_n net thrust, lb

The weight of the airplane was determined from the take-off weight and the amount of fuel used between the take-off and the time of the run. The longitudinal acceleration factor was measured by an accelerometer which is sensitive to 0.0025 g. The angle of attack was obtained from the normal-force angle-of-attack curve for this airplane measured during previous tests.

The gross thrust was calculated from the following isentropic relationships which were derived from reference 3:

$$\frac{F_g}{p_o A} = \frac{2\gamma}{\gamma-1}\left[\left(\frac{p_T}{p_j}\right)^{\frac{\gamma-1}{\gamma}} - 1\right] \text{ for } \frac{p_T}{p_o} < \left(\frac{\gamma+1}{2}\right)^{\frac{\gamma}{\gamma-1}}$$

$$= \left[\frac{2p_T}{p_o}\left(\frac{2}{\gamma+1}\right)^{\frac{1}{\gamma+1}} - 1\right] \text{ for } \frac{p_T}{p_o} \geq \left(\frac{\gamma+1}{2}\right)^{\frac{\gamma}{\gamma-1}}$$

where

p_T tailpipe total pressure, lb/sq ft

p_o free-stream static pressure, lb/sq ft

p_j tailpipe static pressure, lb/sq ft

γ ratio of specific heats (assuming $\gamma = 1.33$ at the tailpipe exit)

F_g gross thrust, lb

A tailpipe area, sq ft

The total pressure in the tailpipe was measured by a single air-cooled, total-pressure probe (fig. 24) mounted in the jet-engine tailpipe, and a uniform distribution of temperature and pressure in the tailpipe was assumed. It was also assumed that the static pressure in the tailpipe exit was equal to free-stream static pressure and there were no nozzle losses.

The net thrust used in the drag equation was obtained from

$$F_n = F_g - \frac{w_a}{g} V$$

where

w_a weight of air through engine, lb/sec

g acceleration due to gravity, ft/sec^2

V airplane velocity, ft/sec

The values of weight of air necessary for the engine for various power settings (engine speed) were obtained from results of the manufacturer's test-stand evaluation of the engine.

REFERENCES

1. Thompson, Jim Rogers, Bray, Richard S., and Cooper, George E.: Flight Calibration of Four Airspeed Systems on a Swept-Wing Airplane at Mach Numbers up to 1.04 by the NACA Radar-Phototheodolite Method. NACA RM A50H24, 1950.

2. Smith, Norman F., and Baals, Donald D.: Wind-Tunnel Investigation of a High-Critical-Speed Fuselage Scoop Including the Effects of Boundary Layer. NACA WR L-733, 1945. (Supersedes NACA ACR L5B01a)

3. Conrad, E. William, and Sobolewski, Adam E.: Altitude-Wind-Tunnel Investigation of J47 Turbojet-Engine Performance. NACA RM E9G09, 1949.

TABLE I.- DIMENSIONS OF TEST AIRPLANE

Wing	
Total wing area (including flaps, aileron, and 65.83 square feet covered by fuselage)	306.10 sq ft
Span	38.90 ft
Aspect ratio	4.943
Taper ratio	0.502
Mean aerodynamic chord	98.75 in.
Sweepback angle	
Leading edge	37°45'
25-percent element	35°15'
Fuselage	
Length	42.75 ft
Depth, maximum	76.6 in.
Width, maximum	85.0 in.
Fineness ratio	6.125
Inlets	
Submerged	
Entrance area (one inlet)	240 sq in.
Length	35.0 in.
Width	8.0 in.
Boundary-layer bleed area	61 sq in.
Boundary-layer bleed height	1.8 in.
Scoop	
Entrance area (one inlet)	215 sq in.
Length	28.0 in.
Width	9.5 in.
Boundary-layer bleed area	34.2 sq in.
Boundary-layer bleed height	1.5 in.

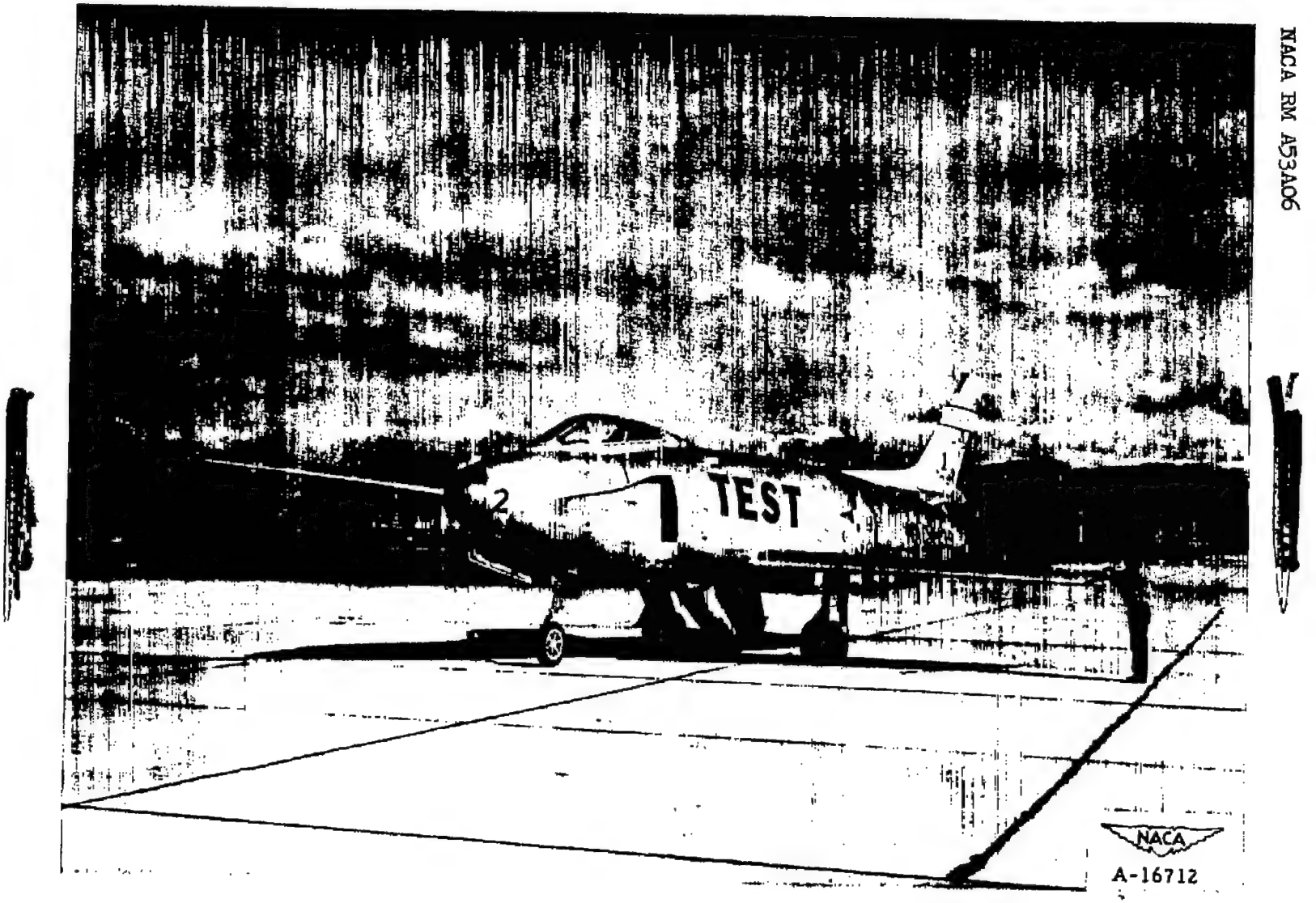

Figure 1.— The test airplane with NACA submerged divergent-wall inlets.

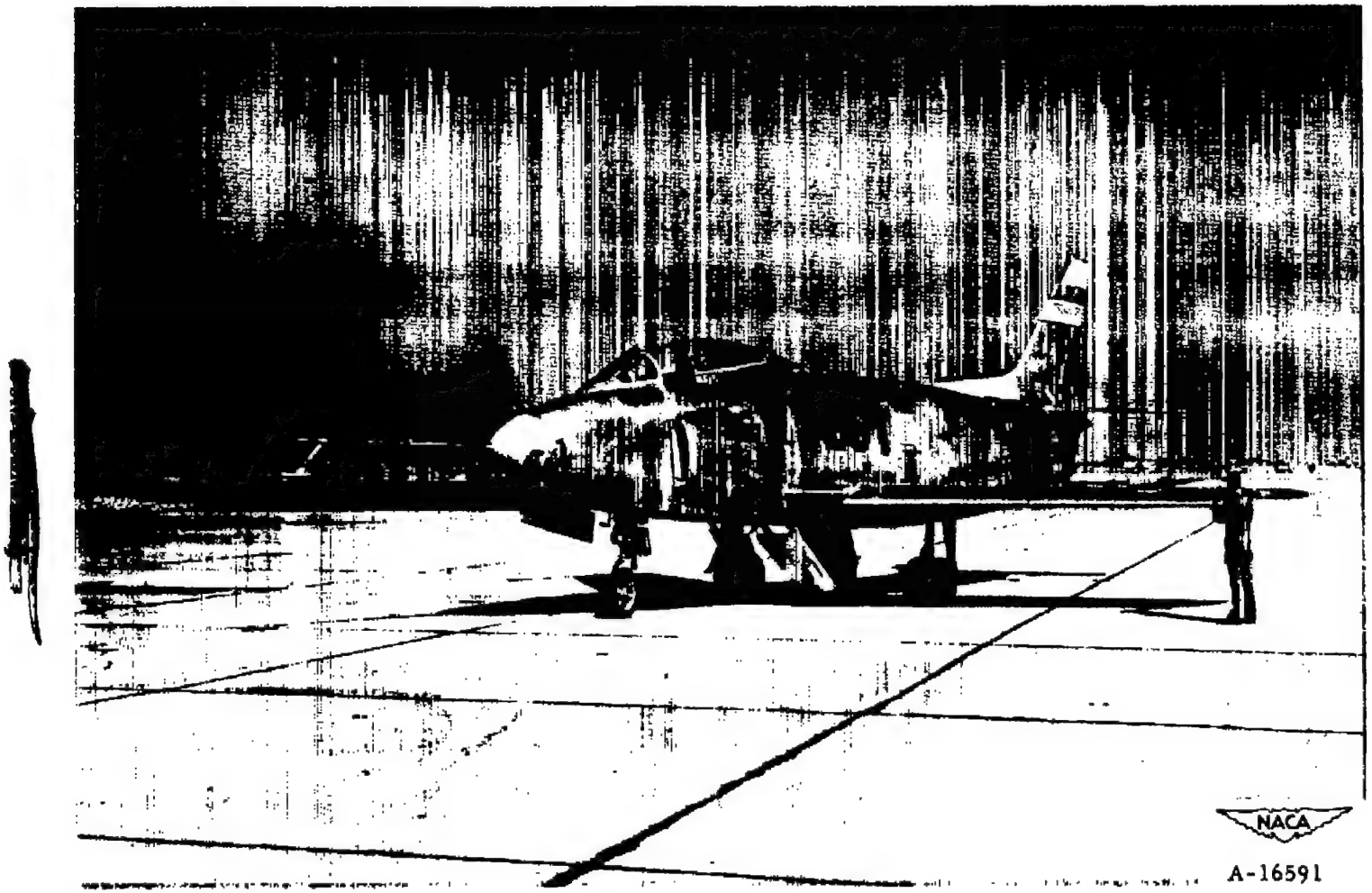

Figure 2.— The test airplane with ram-scoop inlets.

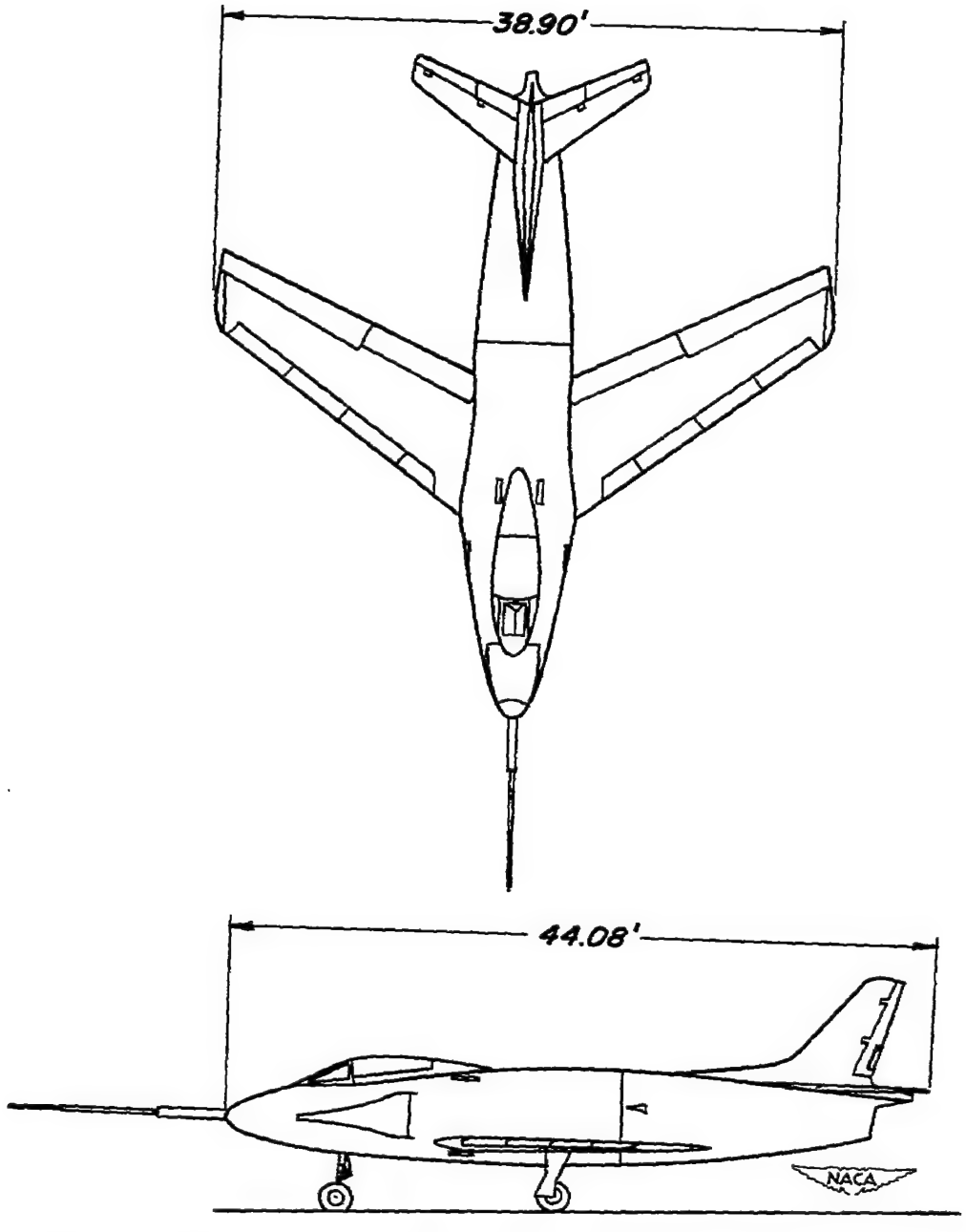

Figure 3.- Two-view drawing of the test airplane with submerged inlet.

[redacted]

(a) Submerged inlet.

(b) Scoop inlet.

Figure 4.— Front views of the two inlets.

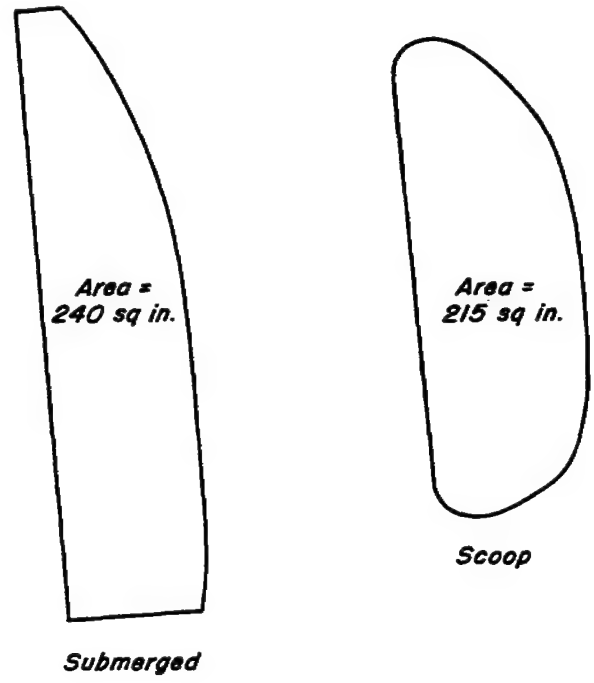

(a) Entrance area.

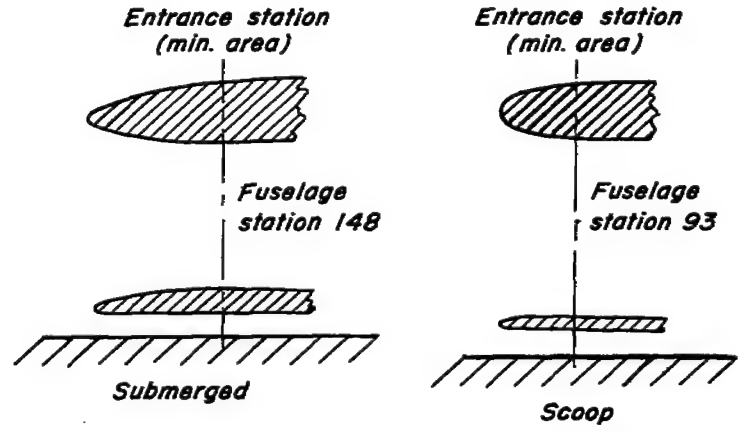

(b) Sketch of inlet profiles.

Figure 5.- Inlet and diffuser geometry.

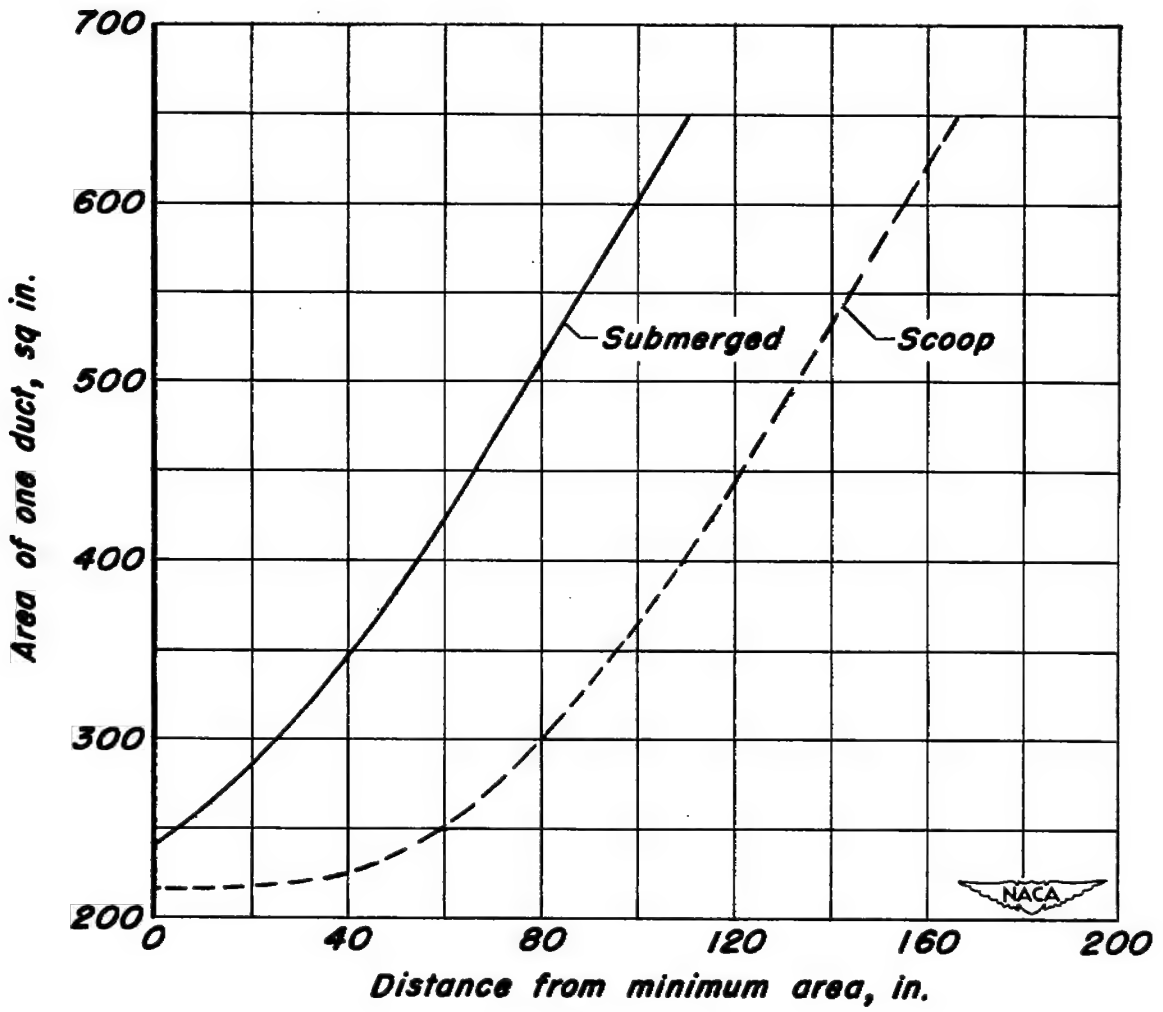

(c) Duct area variation.

Figure 5.- Concluded.

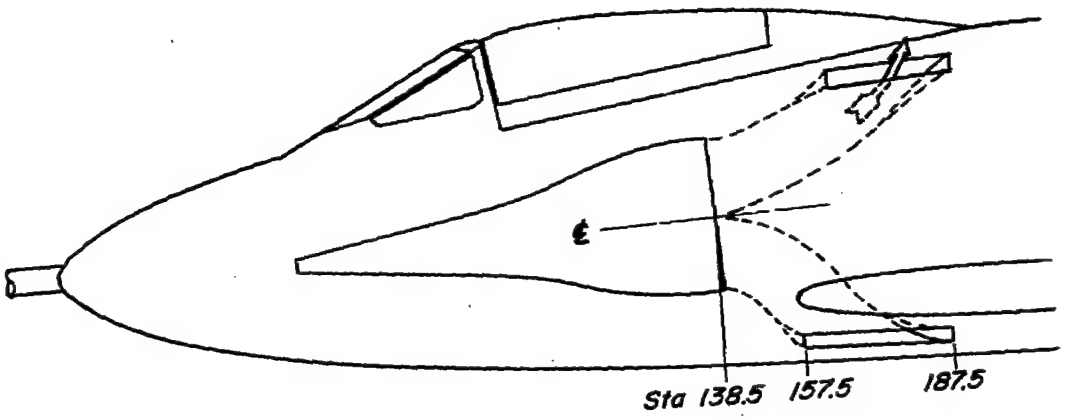

(a) Submerged inlet.

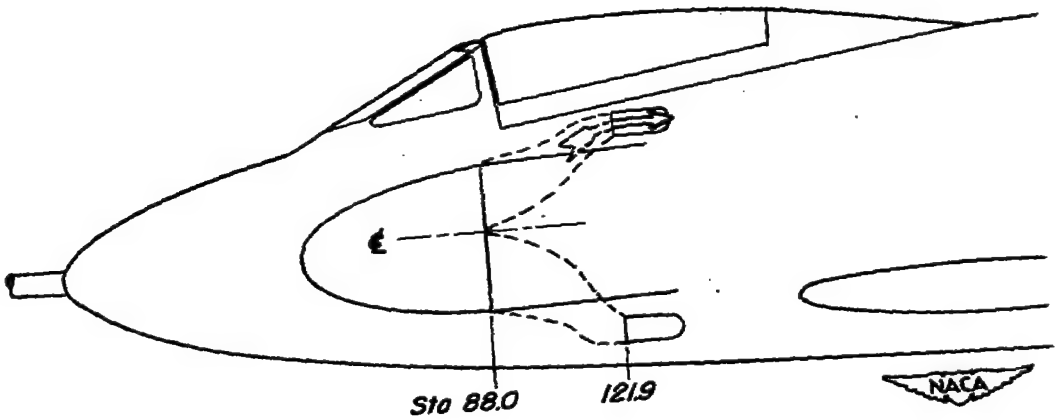

(b) Scoop inlet.

Figure 6.- Inlet location and boundary-layer bleed ducting.

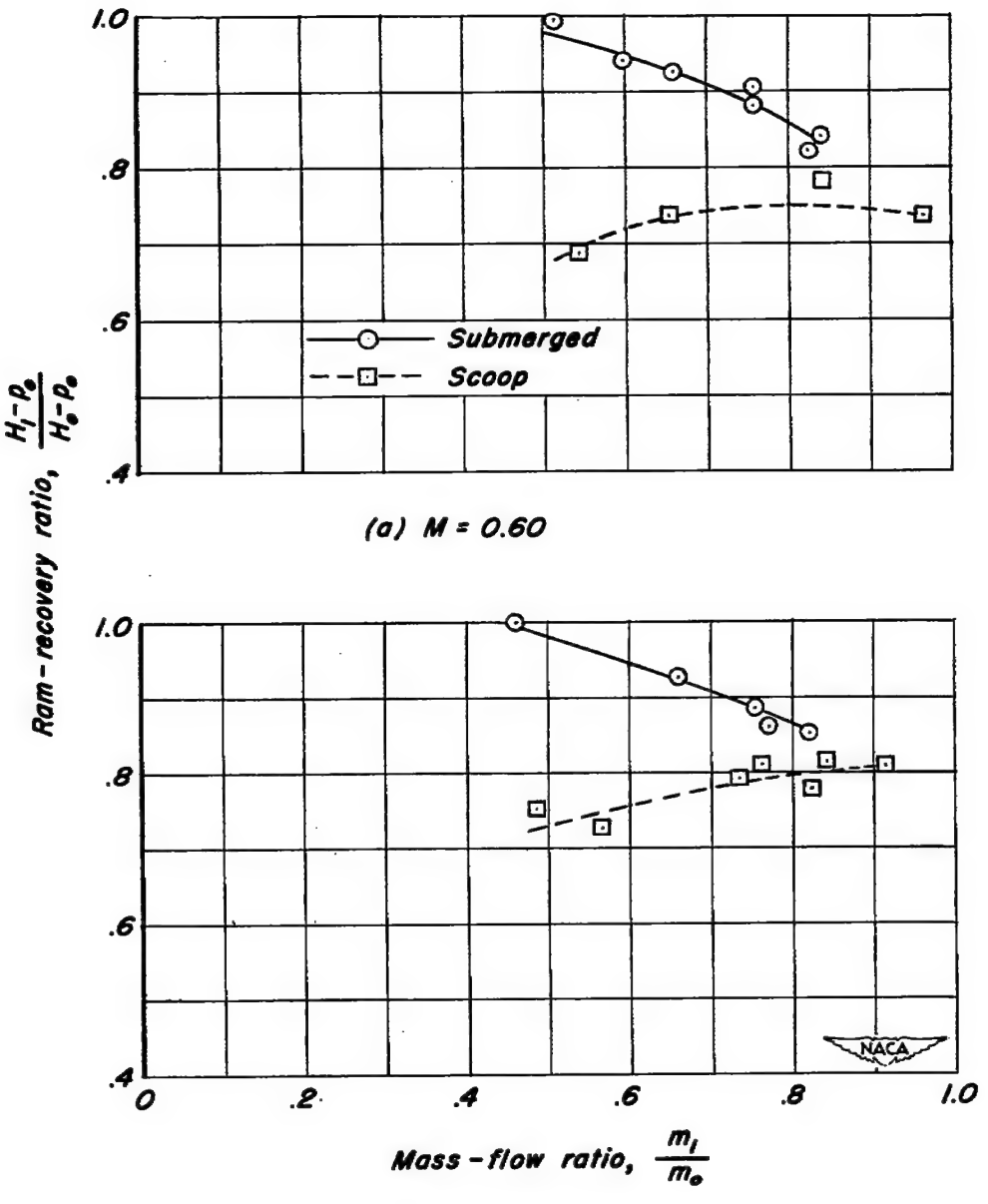

Figure 7.– Typical variations of ram-recovery ratio at the inlet with mass-flow ratio.

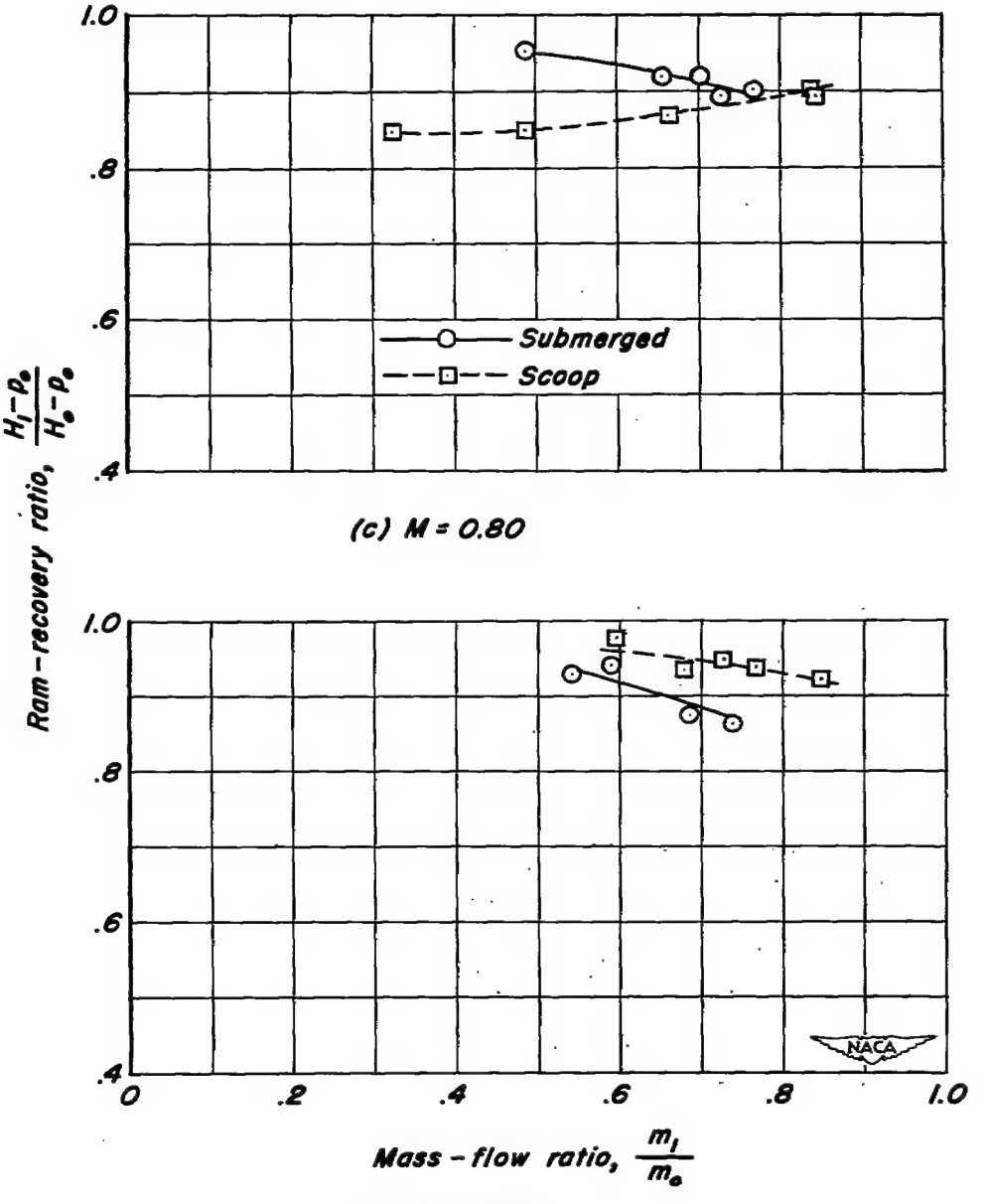

Figure 7.- Concluded.

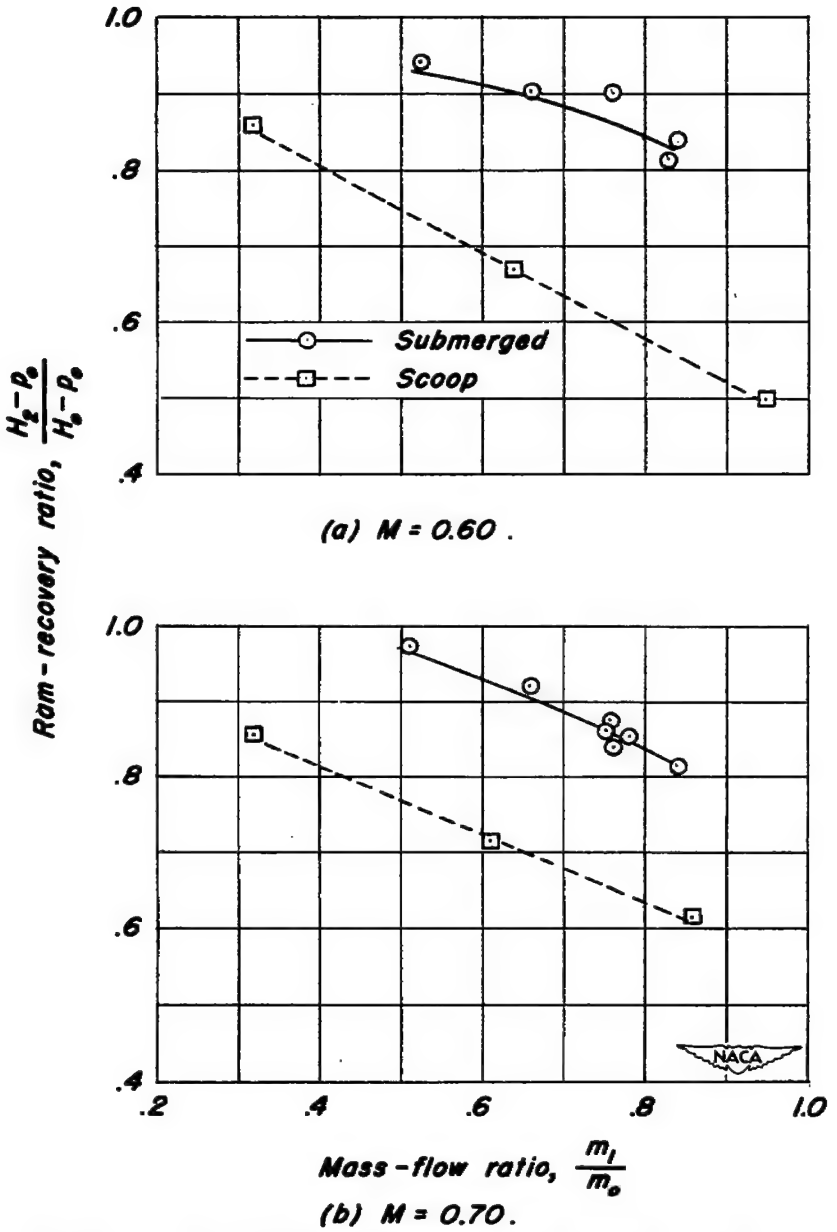

Figure 8.- Typical variation of ram-recovery ratio at the compressor face with mass-flow ratio.

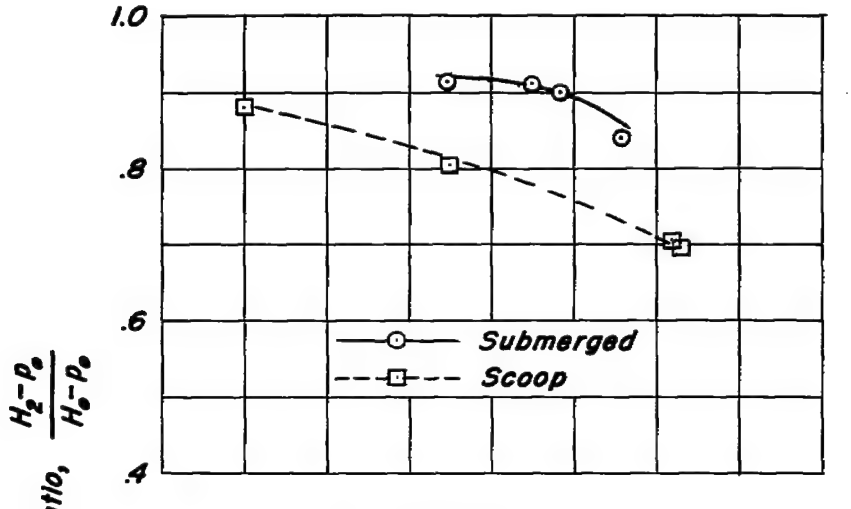

(c) M = 0.80 .

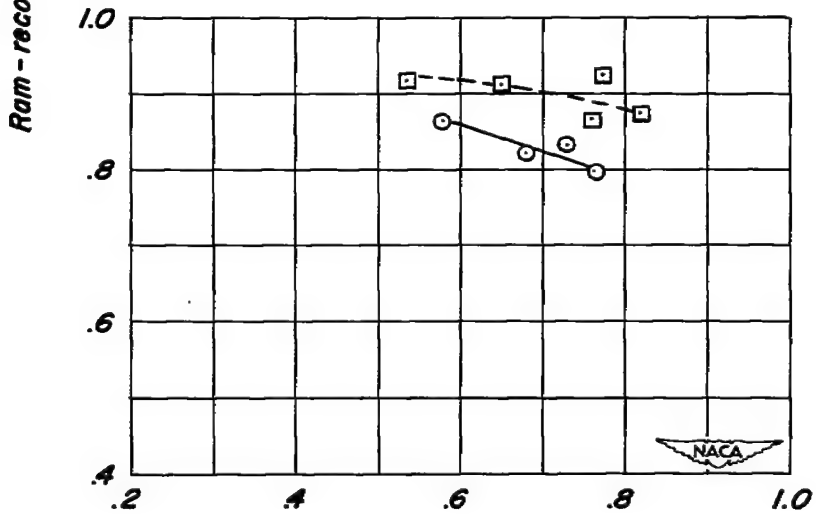

(d) M = 0.90 .

Figure 8.- Concluded.

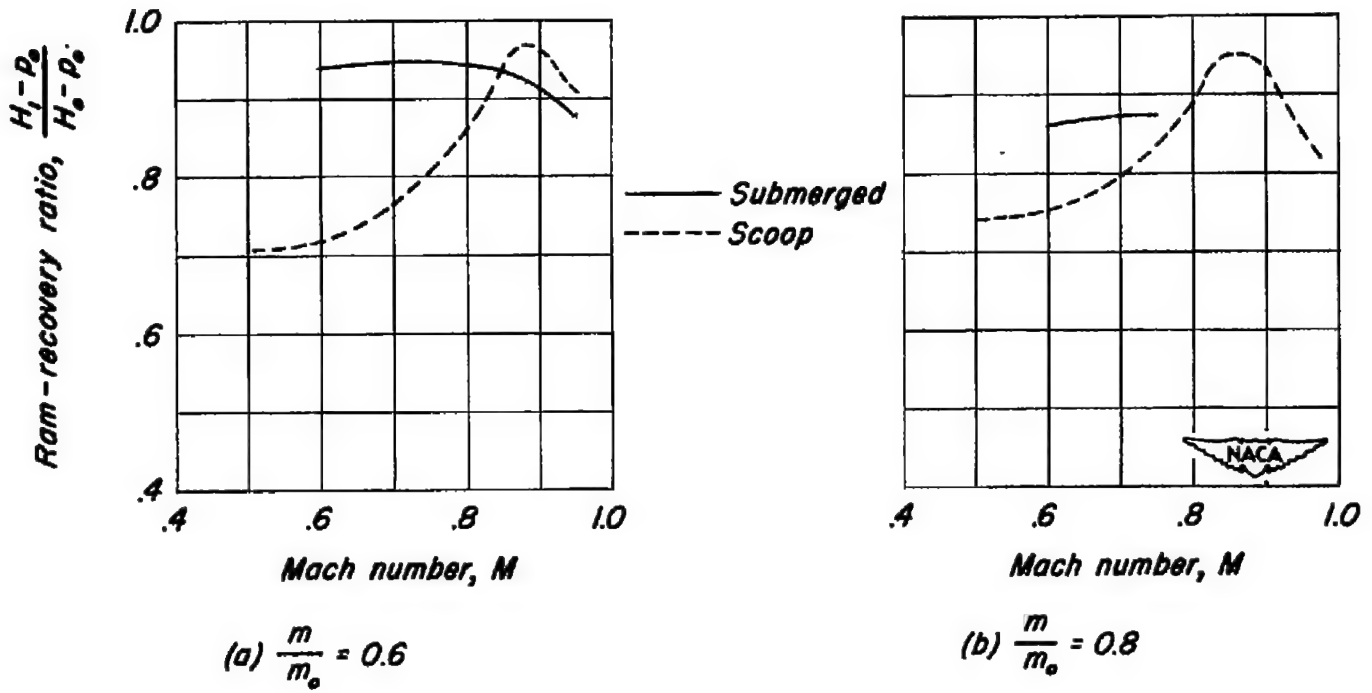

Figure 9.— Variation of ram-recovery ratio at the inlet with Mach number for constant mass-flow ratio for the submerged and scoop inlets.

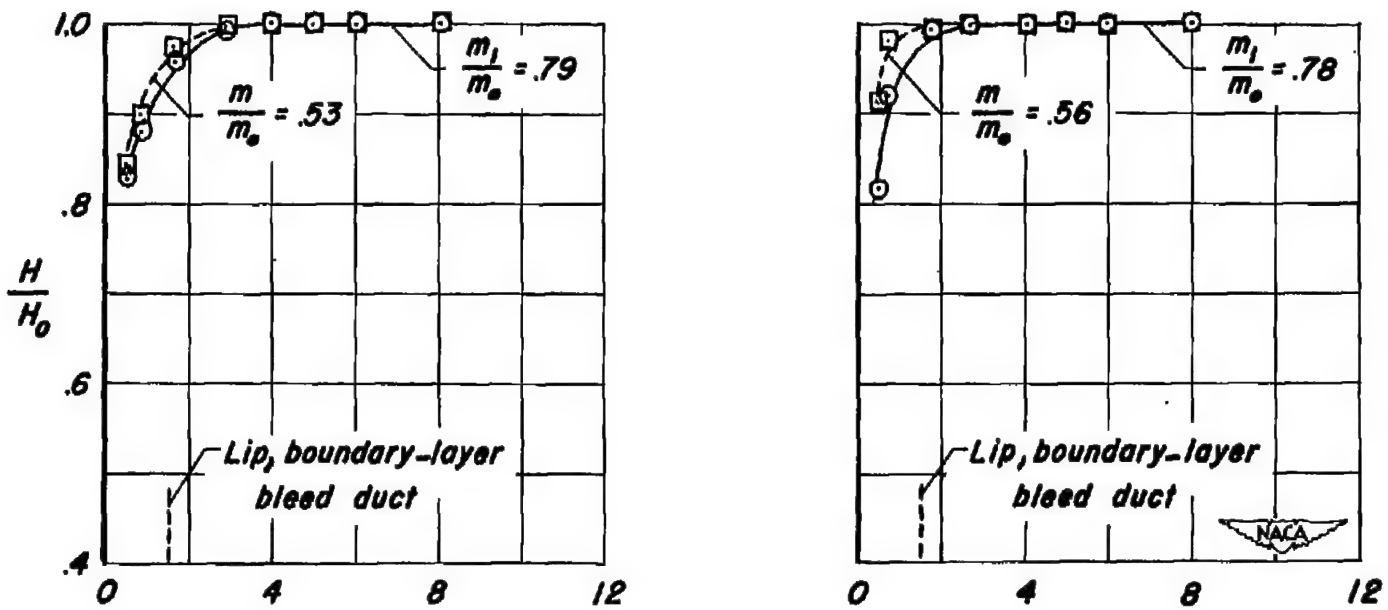

Distance away from fuselage surface, in.

(a) $M \approx 0.90$.

(b) $M \approx 0.70$.

Figure 10.- Variation of total-pressure ratio ahead of scoop inlet with distance away from fuselage surface.

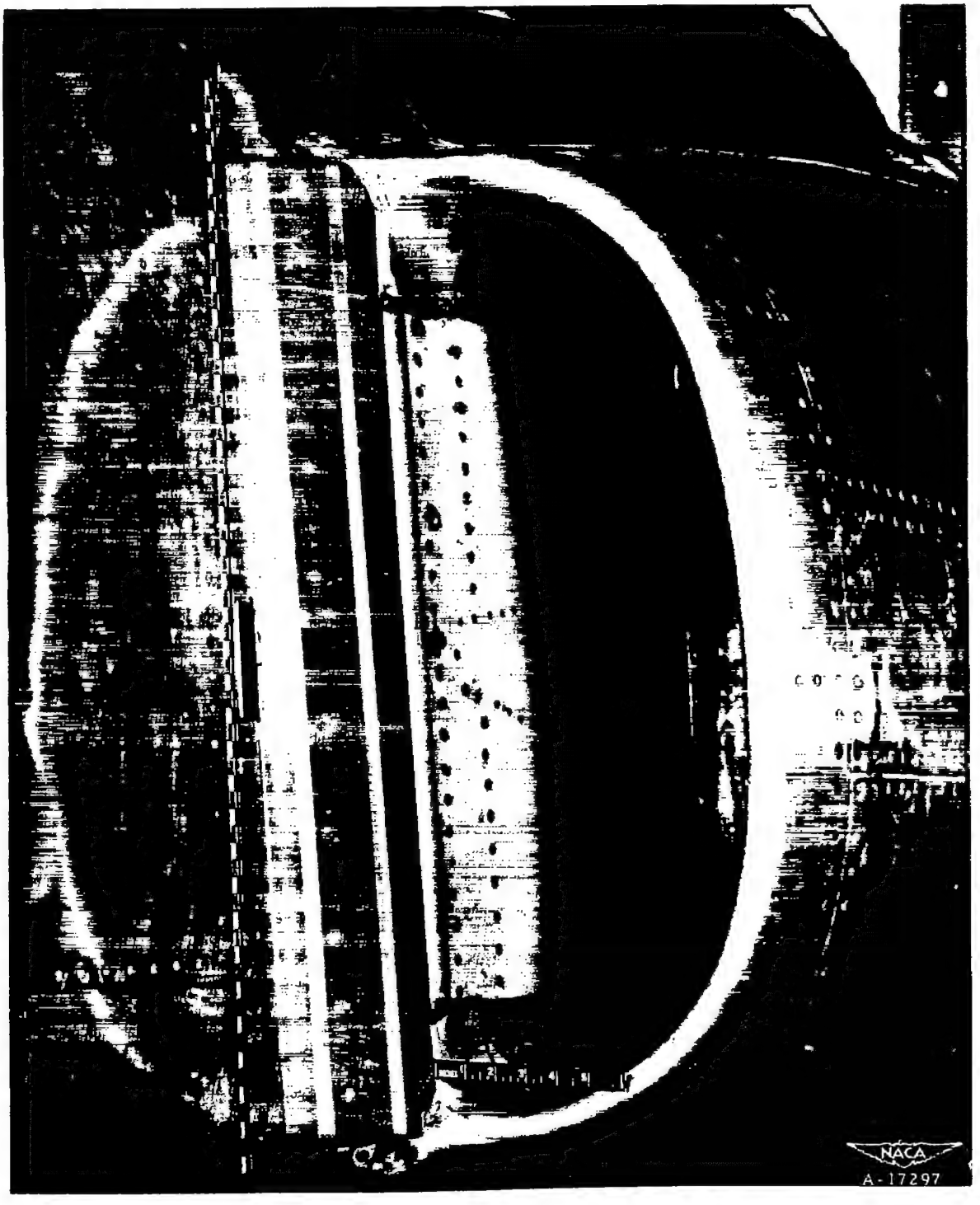

Figure 11.– View of scoop inlet with boundary-layer bleed sealed.

[redacted]

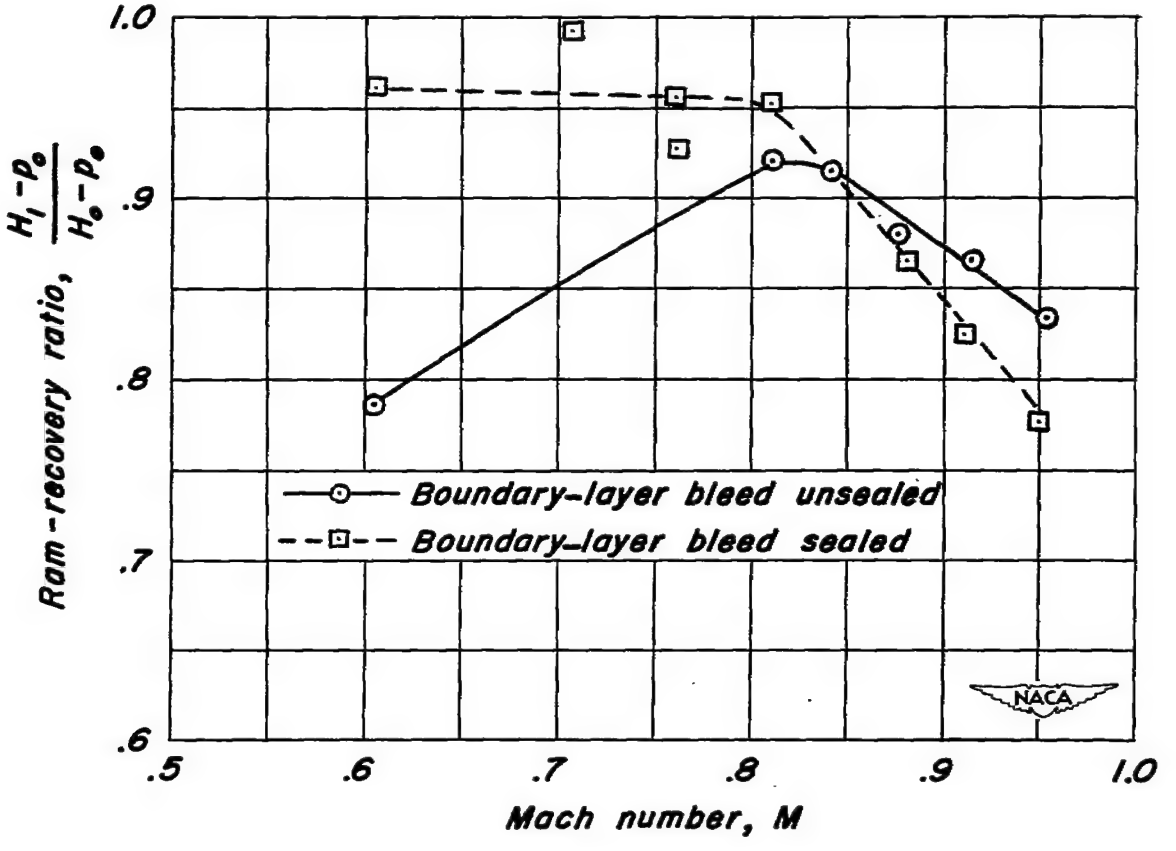

Figure 12.— Variation of ram-recovery ratio at the scoop inlet, determined by a center-line rake, at military power and 25,000 feet altitude. Boundary-layer bleeds sealed and unsealed.

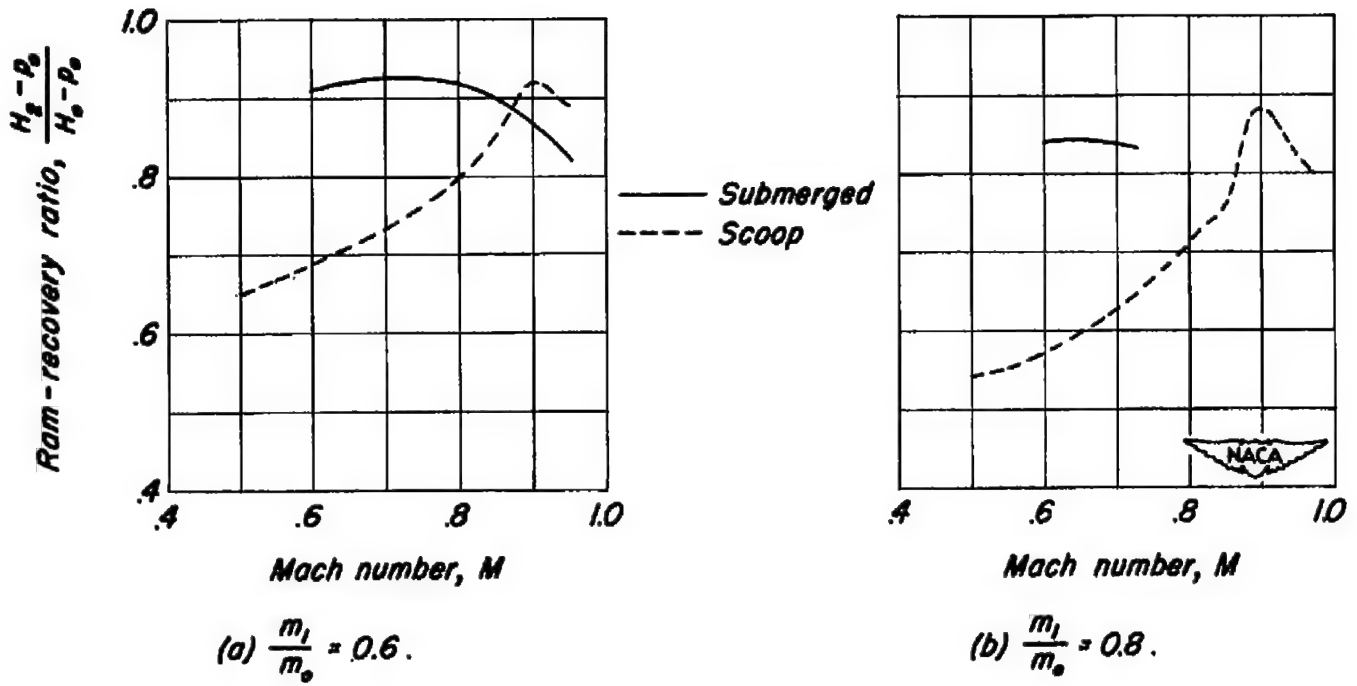

Figure 13.– Variation of ram-recovery ratio at the compressor face with Mach number for constant mass-flow ratio for the submerged and scoop inlets.

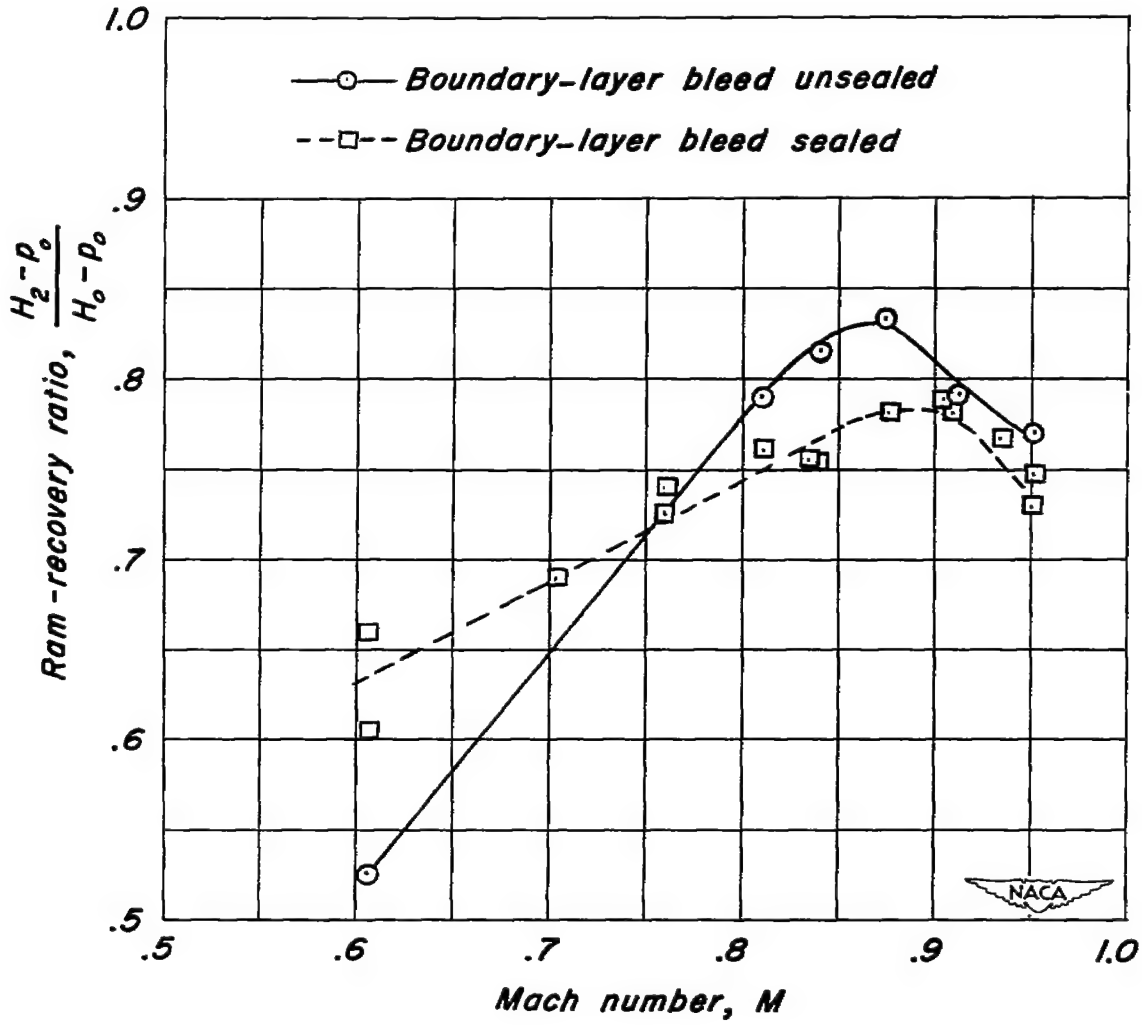

Figure 14.— Variation of the compressor ram-recovery ratio for the scoop inlet at military power and 25,000 feet altitude. Boundary-layer bleeds sealed and unsealed.

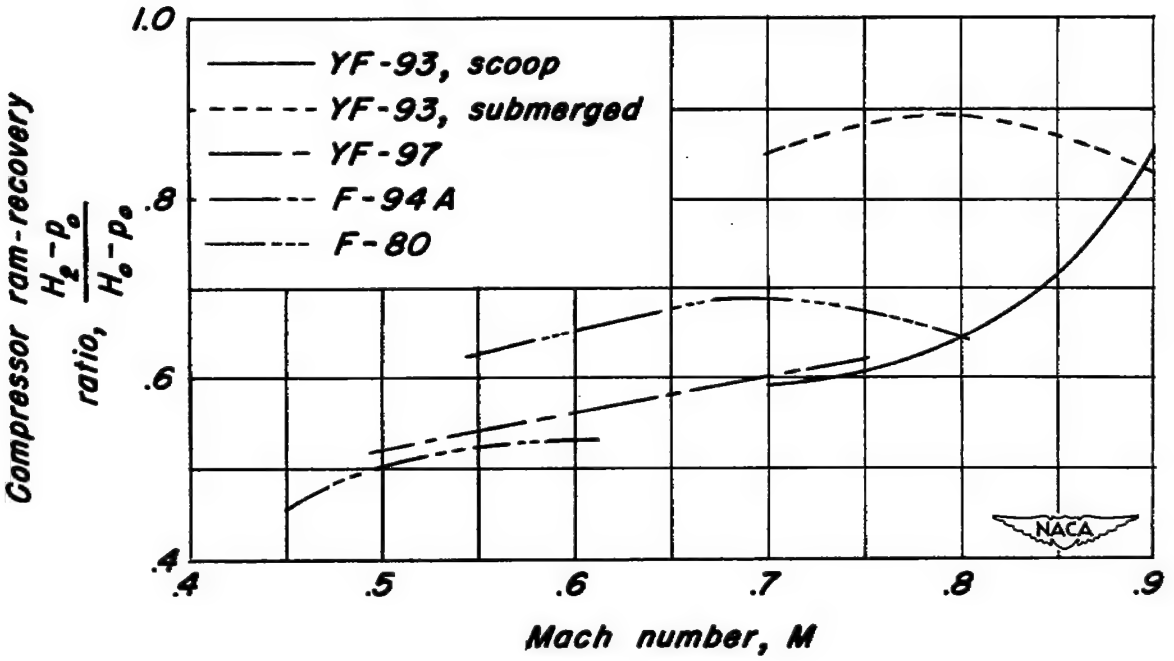

Figure 15.— Comparison of compressor ram-recovery ratio, obtained from flight tests of various airplanes, with Mach number. All with centrifugal compressors.

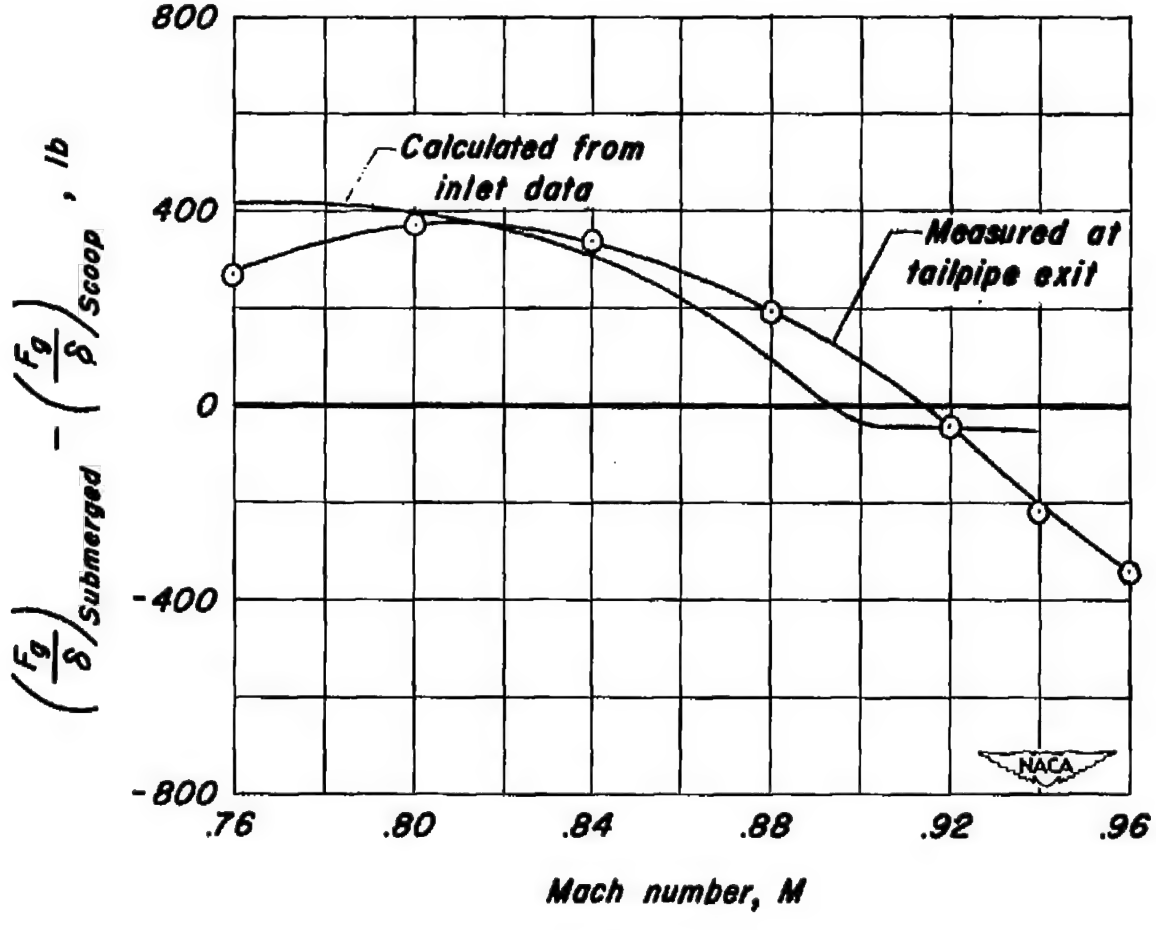

Figure 16.–Variation of the difference in calculated thrust with Mach number for the submerged and scoop inlet systems at military power and 25,000 feet altitude.

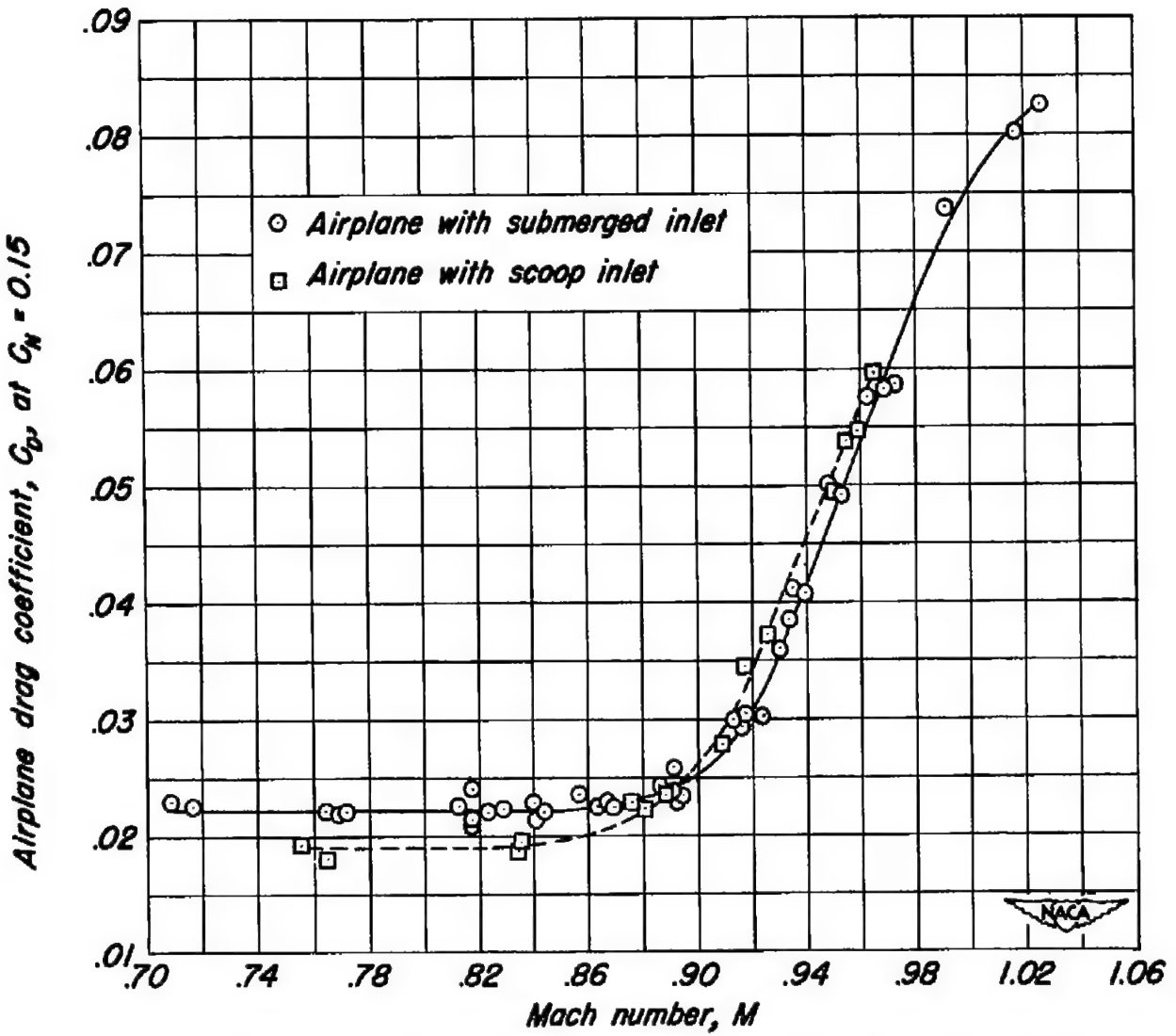

Figure 17.- Variation of total airplane drag coefficient with Mach number.

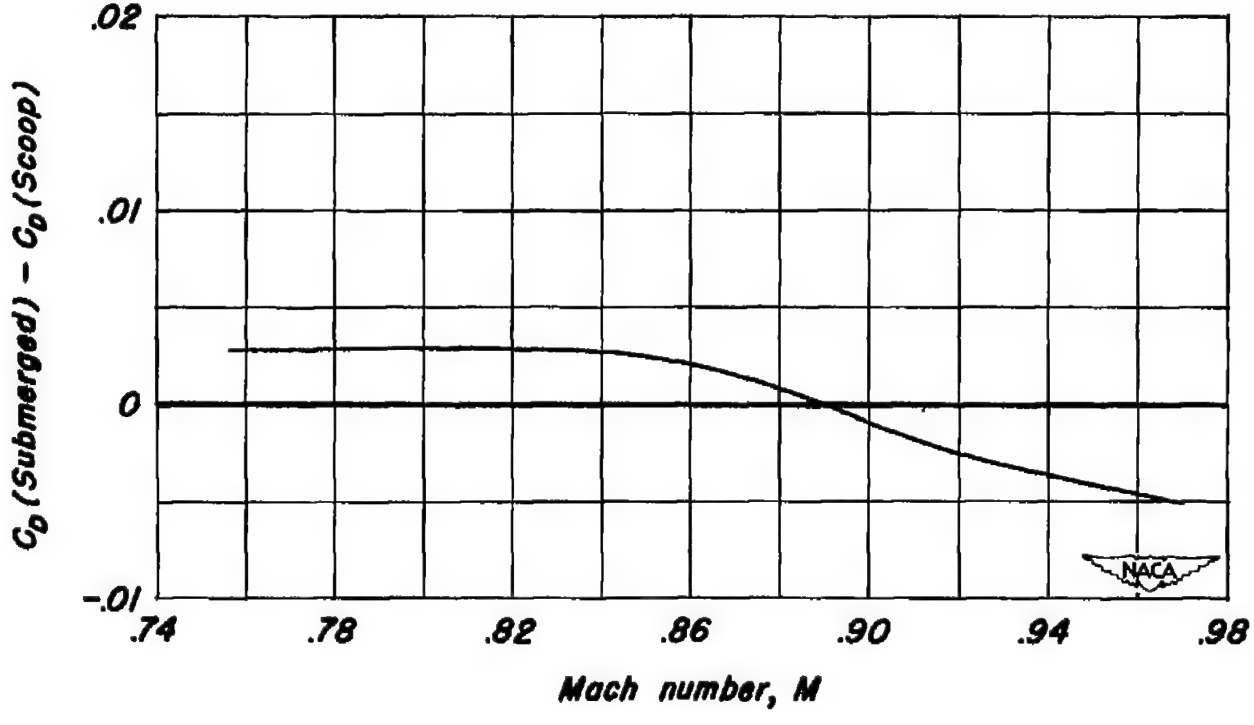

Figure 18.—The variation of incremental airplane drag coefficient with Mach number.

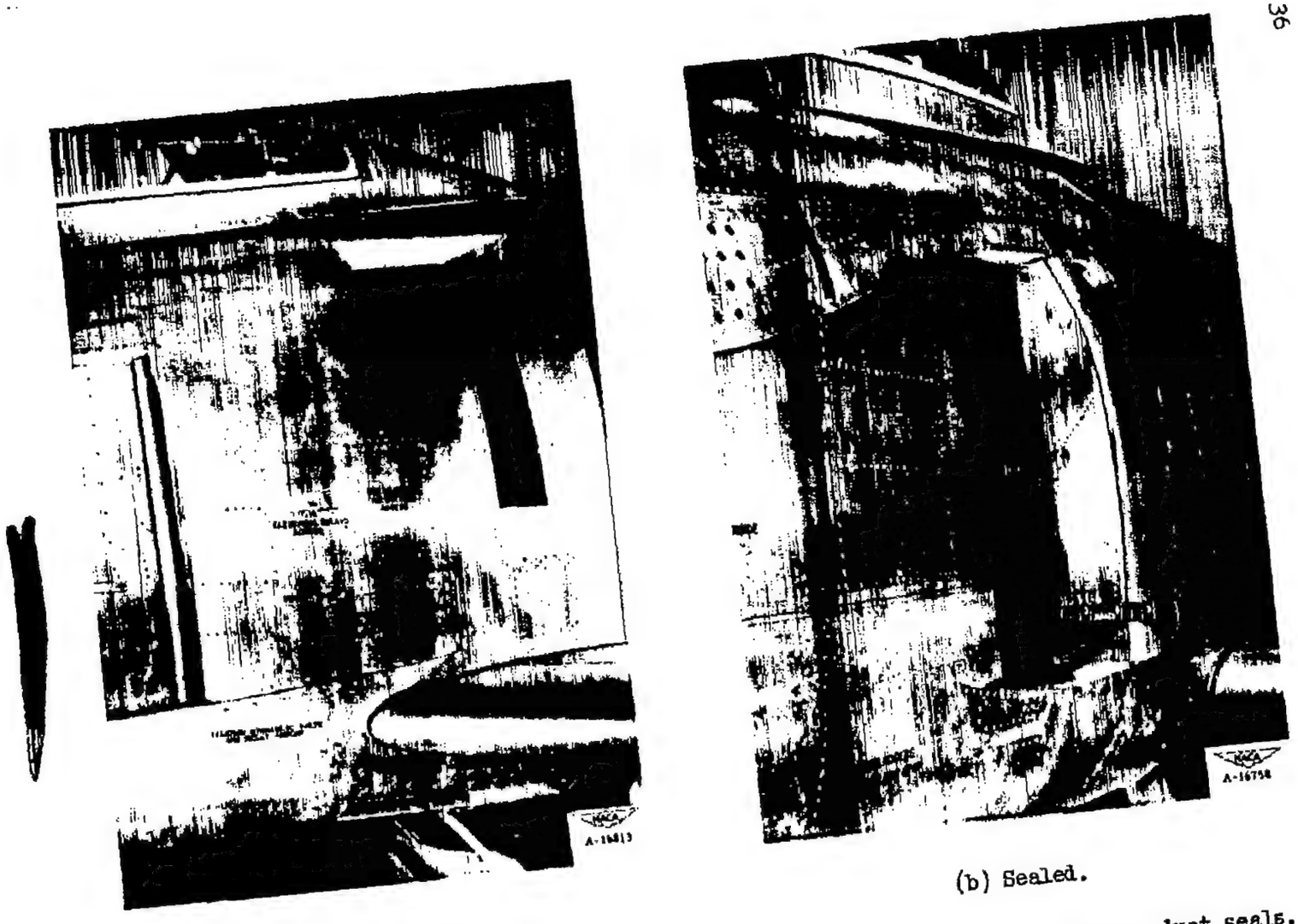

(a) Unsealed.

(b) Sealed.

Figure 19.- Photographs of the submerged inlet showing location of the boundary-layer duct seals.

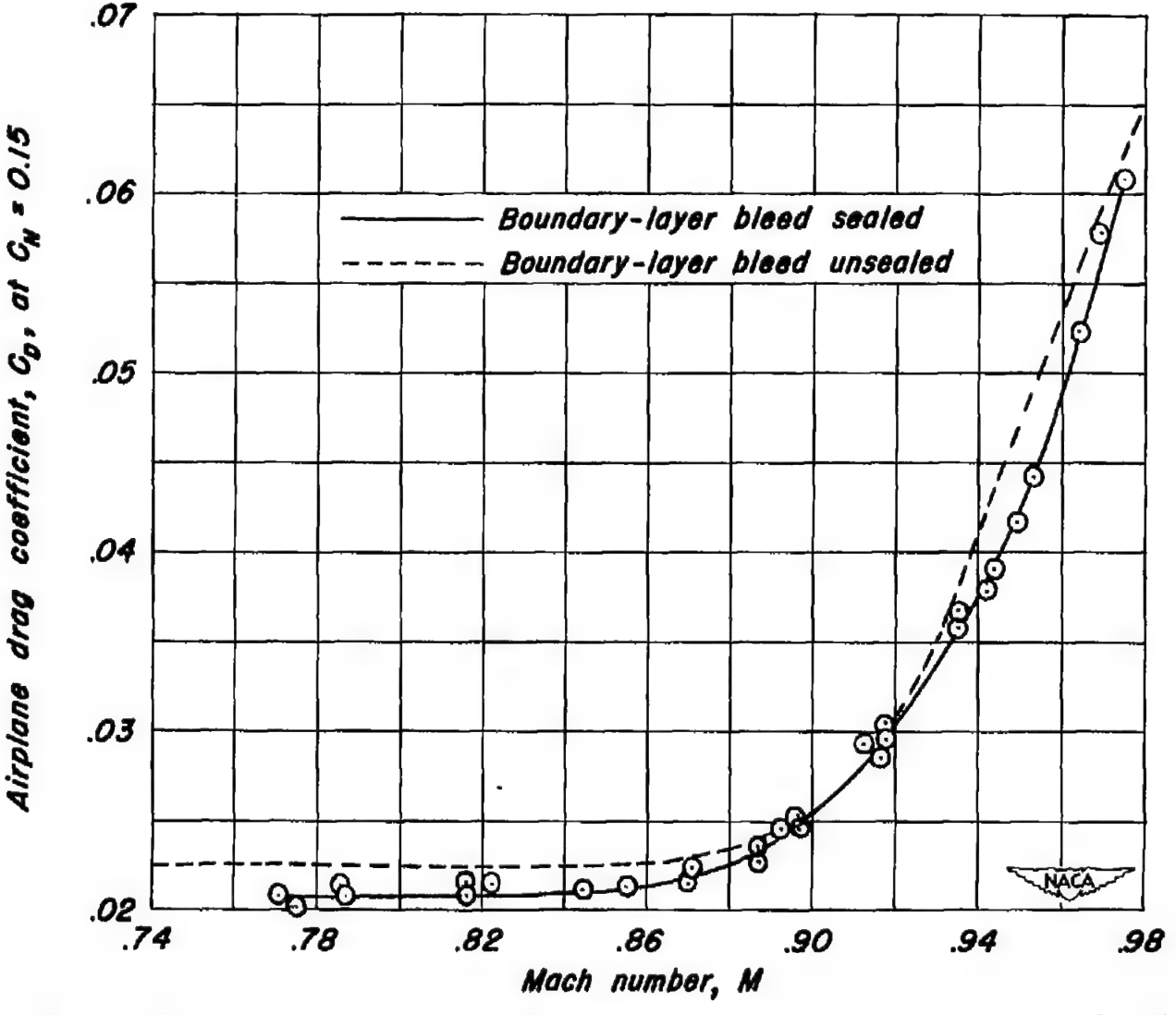

Figure 20.—Airplane drag coefficient variation with Mach number for the submerged inlet with the boundary-layer bleed sealed and unsealed.

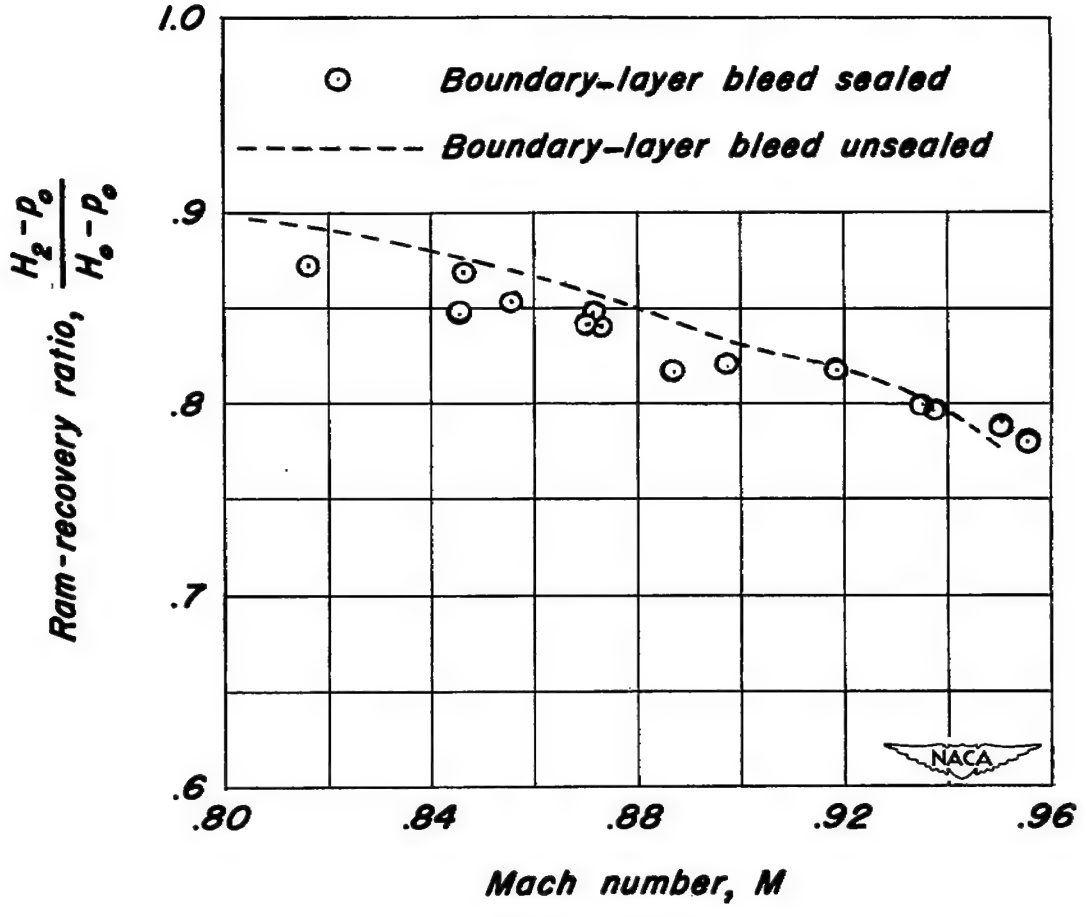

Figure 21.—Variation of ram-recovery ratio at compressor with Mach number for the submerged inlet with the boundary-layer bleed sealed and unsealed at military power and 25,000 feet altitude.

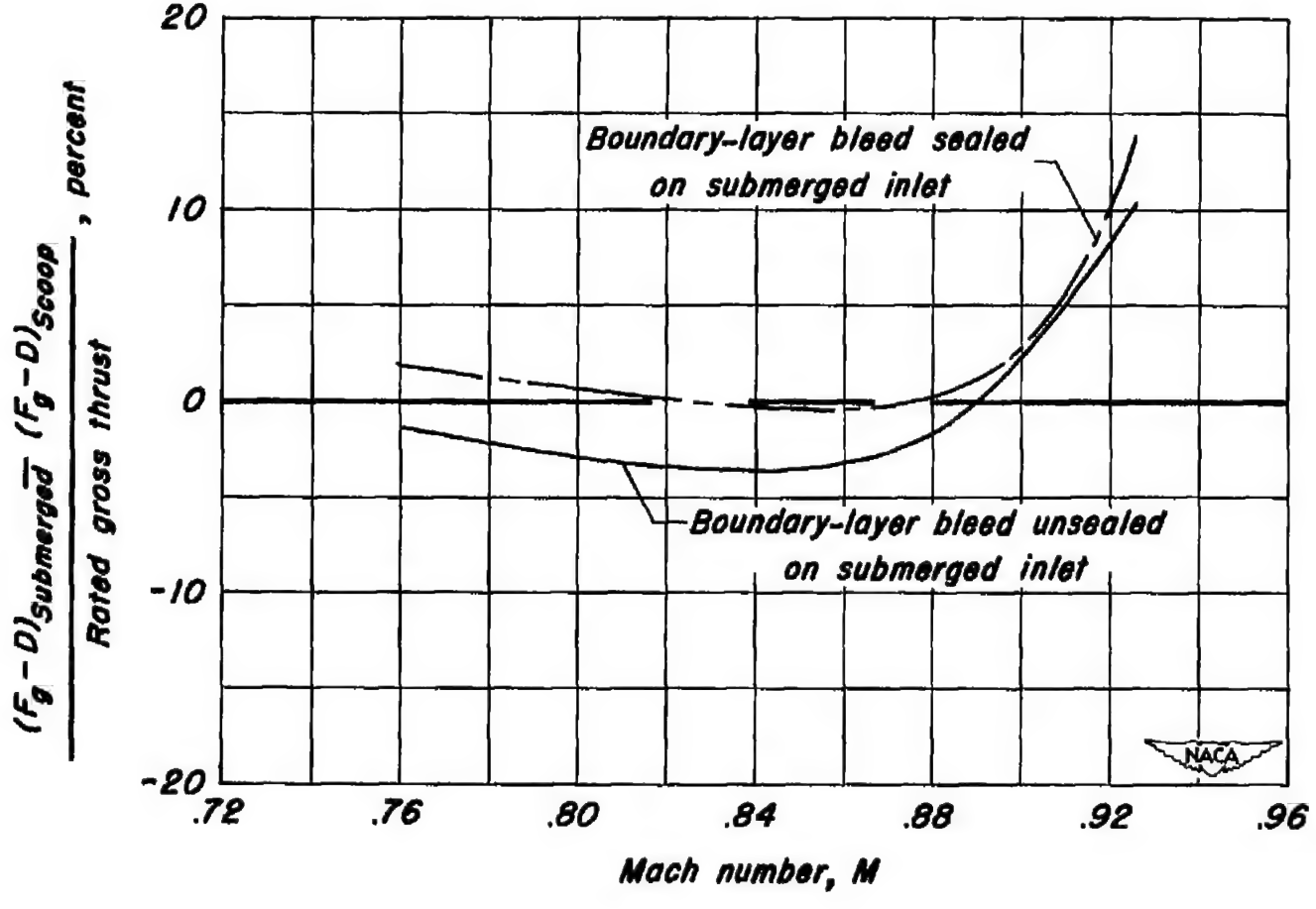

Figure 22.– A comparison of the effectiveness for the two inlets at military power and 25,000 feet altitude.

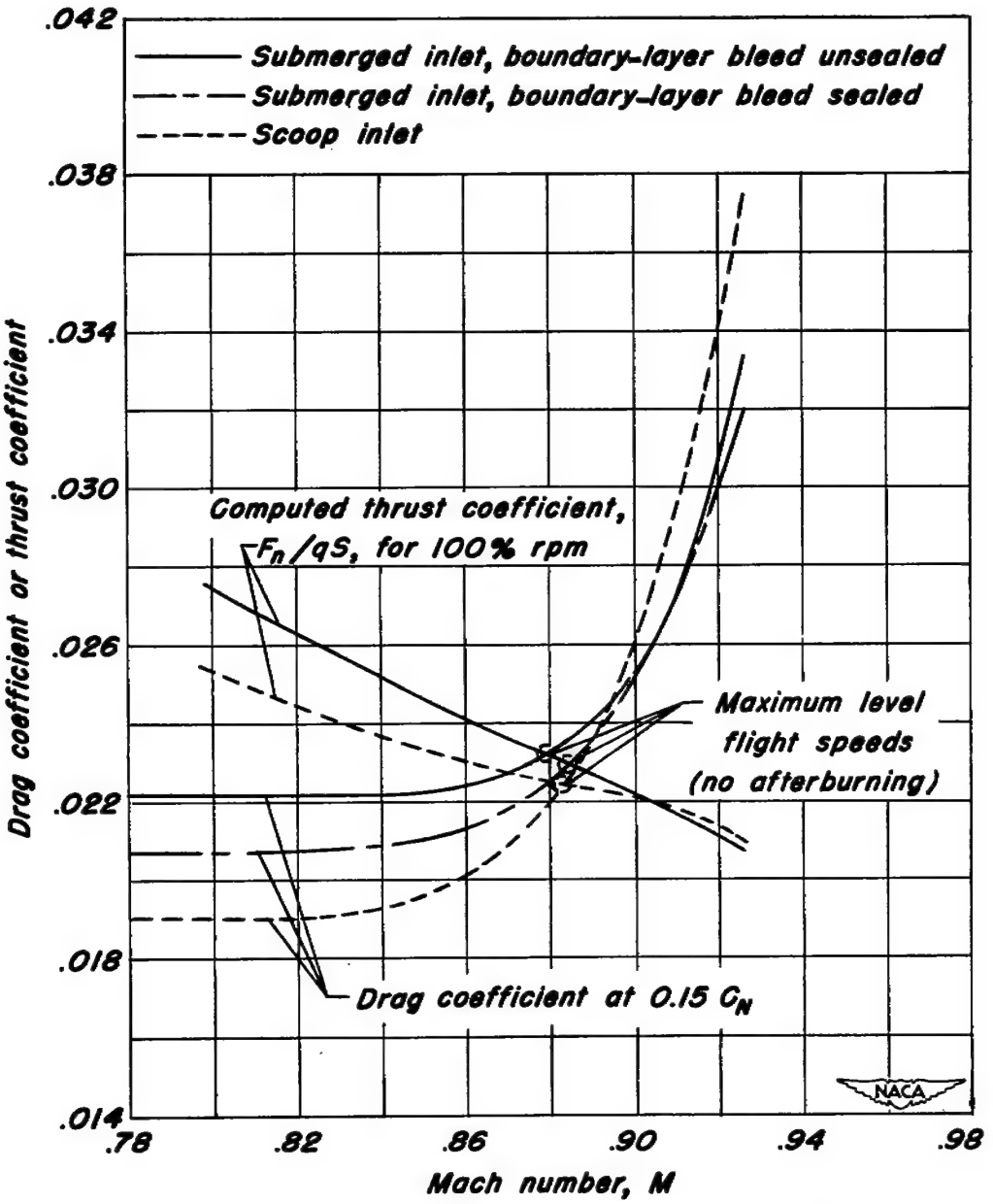

Figure 23.– The variation of the thrust and drag coefficients with Mach number at military power and 25,000 feet altitude.

[redacted]

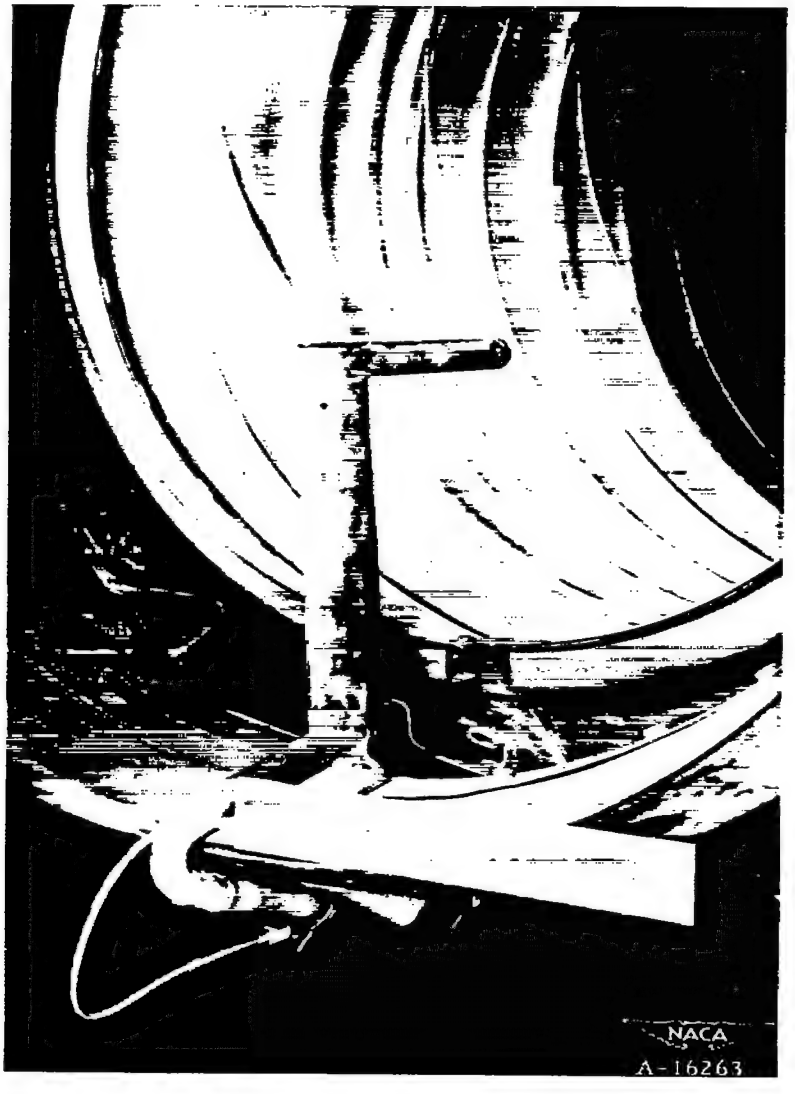

Figure 24.— Single, air cooled, total-pressure probe used for thrust measurements.

[redacted]

NACA-Langley - 3-19-53 -325

~~CONFIDENTIAL~~

ERRATA NO. 1

NACA RM A53A06

A FLIGHT COMPARISON OF A SUBMERGED INLET AND A SCOOP INLET AT TRANSONIC SPEEDS

By L. Stewart Rolls

March 19, 1953

Revised figures 7(a-b), 8(a-b), and 8(c-d), pages 22, 24, and 25, respectively, should be substituted for those in original report. Modifications consist of additional data points and refairing of the curves.

~~CONFIDENTIAL~~

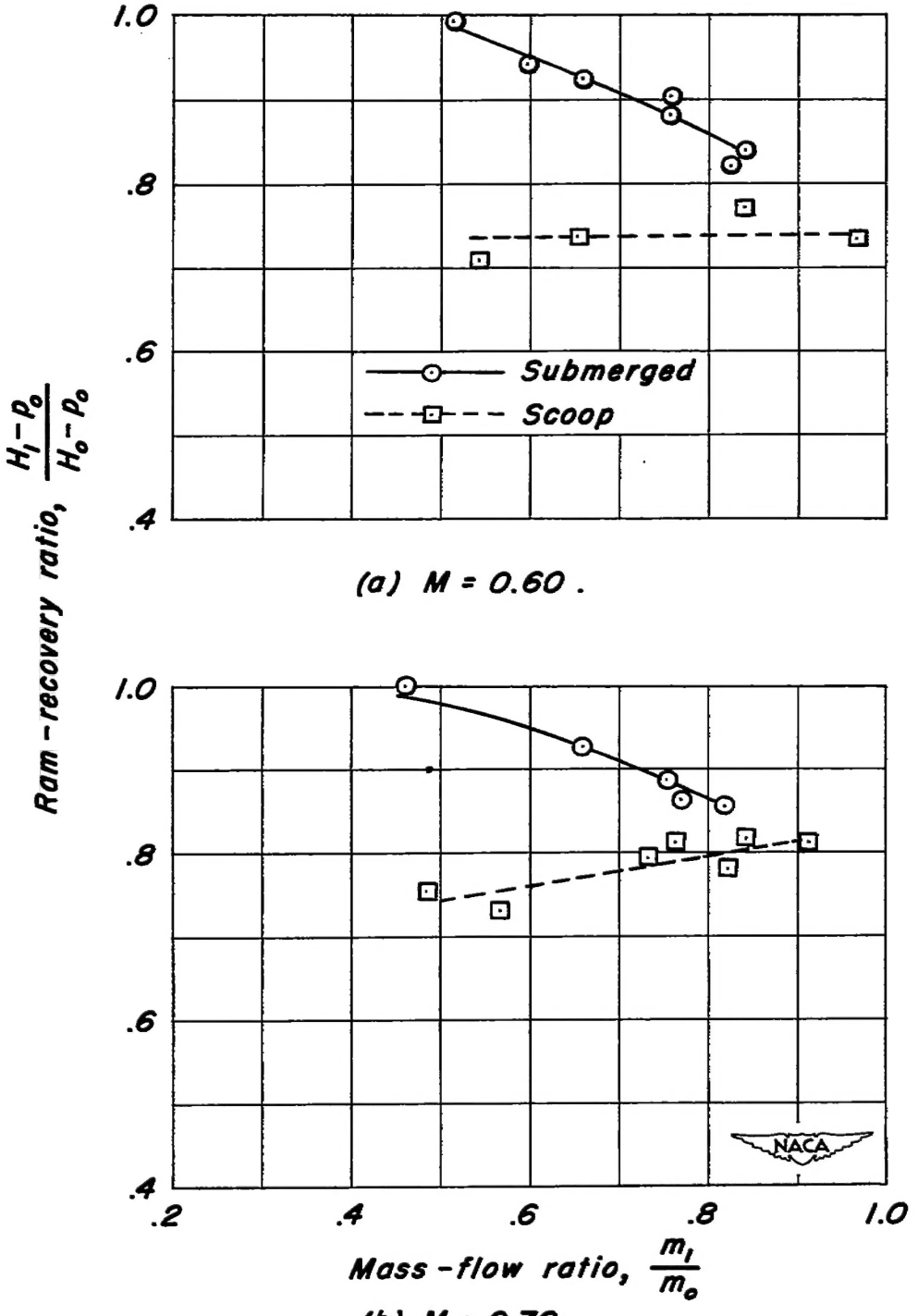

Figure 7.— Typical variations of ram-recovery ratio at the inlet with mass-flow ratio.

[redacted]

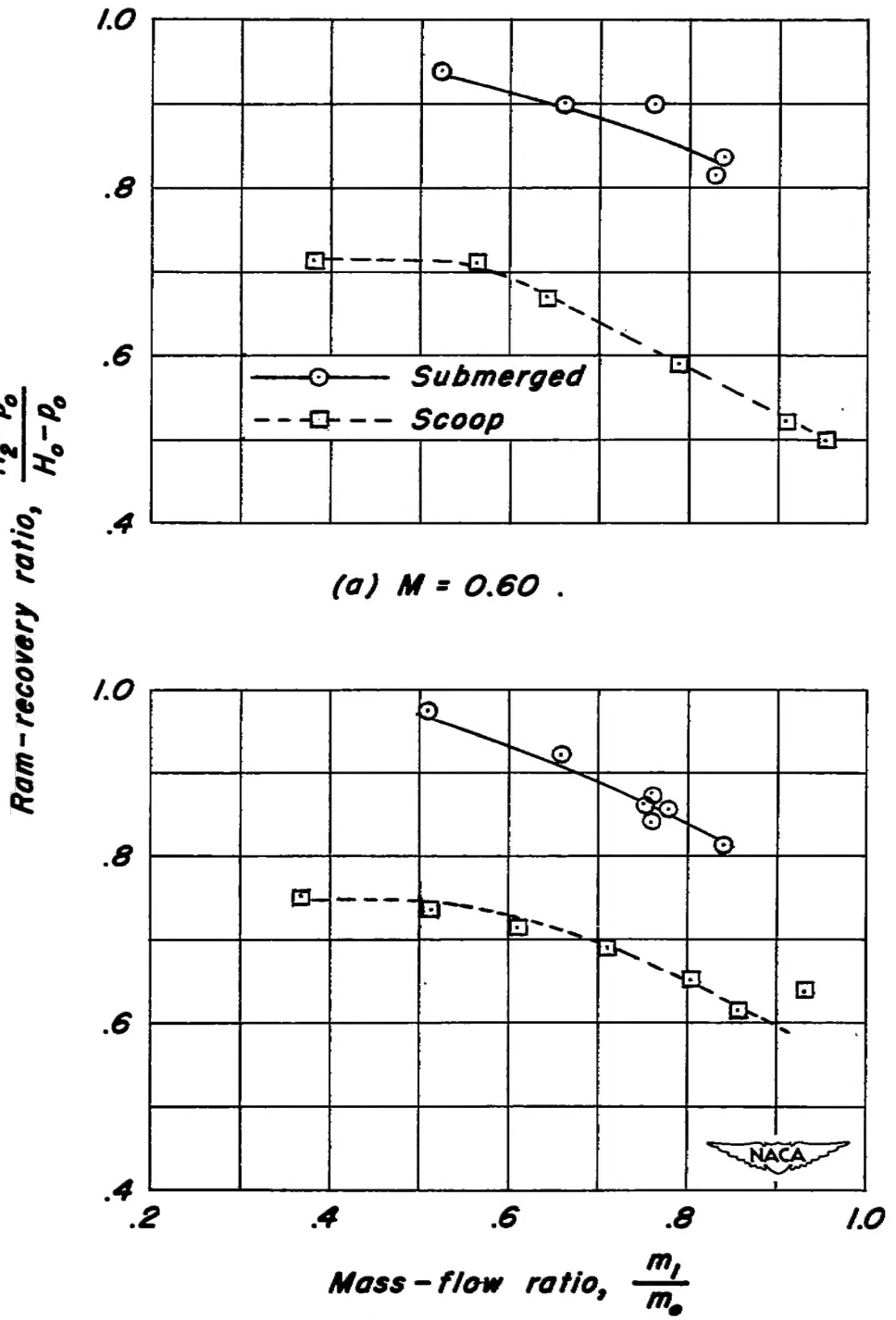

Figure 8.—Typical variation of ram-recovery ratio at the compressor face with mass-flow ratio.

[redacted]

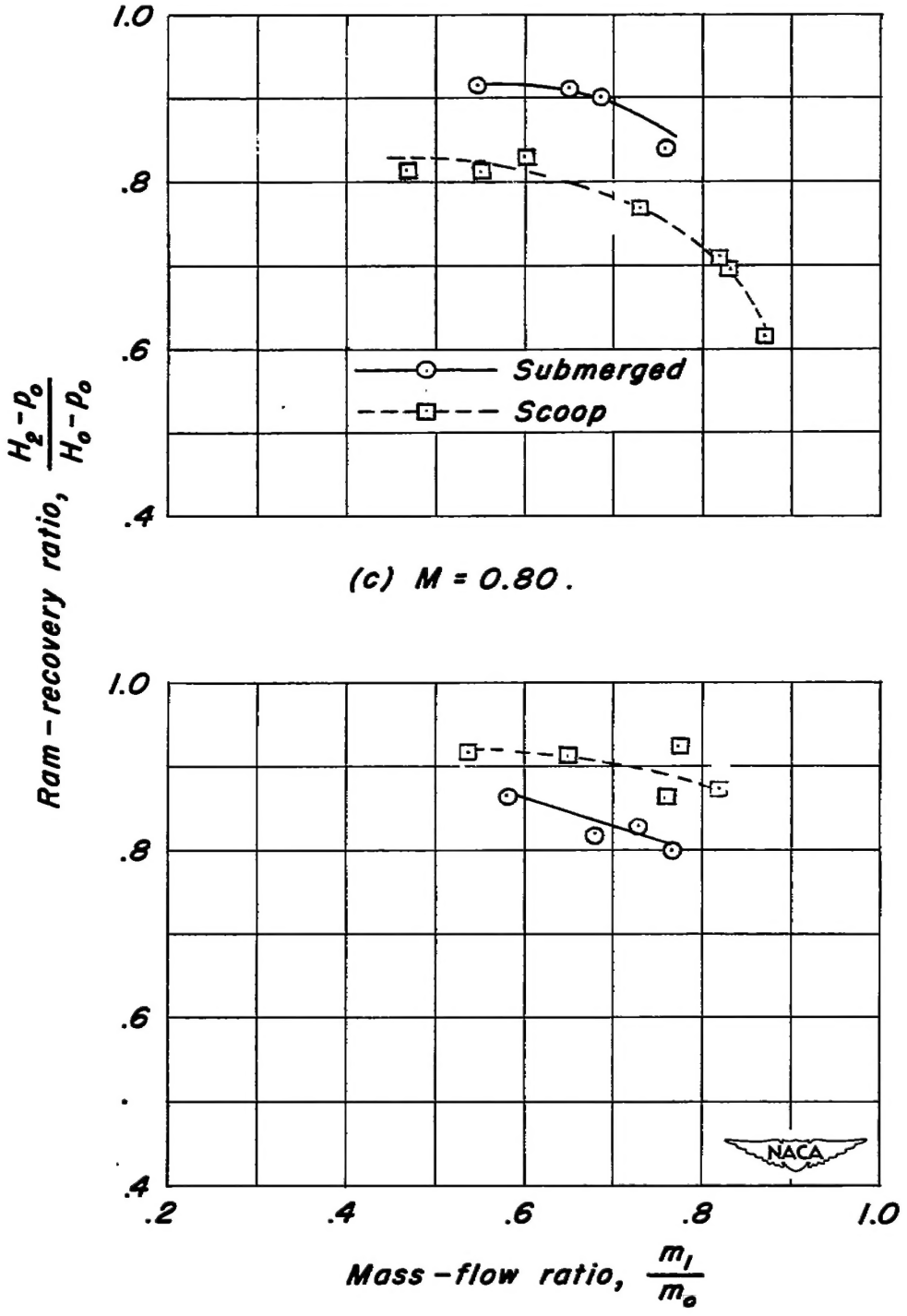

(c) M = 0.80.

(d) M = 0.90.

Figure 8.— Concluded.

[redacted]